Neural Representation of Associative Threat Learning in Pulvinar Divisions, Lateral Geniculate Nucleus, and Mediodorsal Thalamus in Humans

Muhammad Badarnee[1], Zhenfu Wen[1], B. Isabel Moallem[1], Stephen Maren[2,3], and Mohammed R Milad[1*]

[1]Department of Psychiatry and Behavioral Sciences, The University of Texas, Health Science Center at Houston, McGovern Medical School, TX USA.

[2]Beckman Institute for Advanced Science and Technology, University of Illinois Urbana-Champaign, Urbana, IL

[3]Department of Psychology, University of Illinois Urbana-Champaign, Champaign, IL

***Corresponding Author:**

Mohammed R Milad, PhD

Department of Psychiatry and Behavioral Sciences

UTHealth, McGovern Medical School

1941 East Road, BBSB - 2118

Houston, Texas 77054

mohammed.r.milad@uth.tmc.edu

Abstract

Understanding the neural mechanisms underlying associative threat learning is essential for advancing behavioral models of threat and adaptation. We investigated distinct activation patterns across thalamic pulvinar divisions, lateral geniculate nucleus (LGN), and mediodorsal thalamus (MD) during the acquisition of associative threat learning in the MRI. We revealed parallel thalamic learning systems within the anterior pulvinar and MD, supporting distinct mechanisms of automatic survival vs. more deliberate learning. Additionally, our findings support a novel hierarchical pulvinar model during fear conditioning: the medial pulvinar mediates basic threat information from the inferior and lateral divisions to the anterior pulvinar for integrative learning. Pulvinar divisions and MD support extinction learning. These regions also process salience and modulate safe/threat memory expression during extinction recall and threat renewal. The LGN sustains feedforward processing of anticipated visual input throughout all threat phases. This study extends dominant brain models of threat learning and memory, reframing our understanding of distinct thalamic roles in these psychological processes.

Keywords: Thalamus; Pulvinar; Lateral geniculate nucleus; Mediodorsal thalamus; Threat learning; Conditioning; Extinction; Recall extinction; Threat renewal; Emotional memory.

Introduction

Over a century ago, Ivan Pavlov provided foundational behavioral evidence for associative learning, demonstrating that pairing a neutral stimulus with an unconditioned stimulus could elicit a conditioned response(Pavlov, 1904). This discovery laid the groundwork for modern learning theories and has been particularly influential in understanding how humans learn to associate neutral stimuli with threats, a process known as associative threat learning. This survival-oriented learning plays a key role in shaping a broad range of behavioral and emotional responses, such as avoidance, decision-making under threats, and fear regulation(Badarnee et al., 2025; Kolling et al., 2014; Korn and Bach, 2019, 2018; Milad et al., 2013). Research on the neural mechanisms underlying associative threat learning has primarily focused on brain regions involved in emotional regulation, such as the amygdala, hippocampus, and prefrontal cortex (PFC)(Fullana et al., 2015; Krasne et al., 2021; Milad and Quirk, 2012; Vuilleumier et al., 2003). More recently, the thalamus has received growing attention in threat learning(Lithari et al., 2015; Penzo et al., 2015; Ramanathan et al., 2018; Ramanathan and Maren, 2019; Ratigan et al., 2023; Totty et al., 2023), since its role has been reconsidered beyond the traditional view of a mere relay station. Yet, the distinct contribution of this complex structure to associative threat learning remains poorly understood.

The thalamus is a hub structure in the mammalian brain that plays multiple critical roles, ranging from basic sensory processing to higher-order functions and threat learning(Halassa and Sherman, 2019; Hummos et al., 2022; Hwang et al., 2017;

Saalmann and Kastner, 2011; Sherman, 2016, 2007). It has long been proposed that threat detection is mediated by the pulvinar and the lateral geniculate nucleus (LGN)(Carr, 2015; Pessoa and Adolphs, 2010; Silverstein and Ingvar, 2015), two major nuclei of the visual thalamus(Arcaro et al., 2015; Casanova and Chalupa, 2023; Takakuwa et al., 2021). The pulvinar projects directly to the amygdala and is believed to subconsciously facilitate rapid survival reactions to threats via a subcortical path ('low road')(Carr, 2015; Pessoa and Adolphs, 2010; Rafal et al., 2015; Wei et al., 2015). The LGN, on the other hand, is part of a slower but more accurate neural pathway, connecting peripheral information to cortical regions for comprehensive processing ('high road'). Additionally, the involvement of the mediodorsal thalamus (MD) in threat learning has also been proposed(Lee and Shin, 2016; Lee et al., 2011). Although this nucleus is not typically classified as part of the visual thalamus, it serves as a high-order region reciprocally connected to the amygdala and PFC while playing a critical role in executive functions(Hwang et al., 2020; Li et al., 2022; Mukherjee et al., 2021; Wolff and Halassa, 2024).

The general implication of these nuclei in threat processing has been demonstrated in primates and rodent models. It has been shown that exposing primates to snake images elicited increased neuronal firing within the pulvinar(Le et al., 2013). Excitation of neurons within the LGN enhanced the acquisition of eyeblink conditioning in rodents(Halverson and Freeman, 2010). Inhibiting this nucleus was associated with impaired conditioned responses(Shi and Davis, 2001; Steinmetz et al., 2013), and activating GABA neurons in the LGN reduced freezing response to an overhead dark shadow that mimics a real-world

predator in rats(Salay and Huberman, 2021). Reduced freezing was also observed after MD lesions(Li et al., 2004) and when the connections with the anterior cingulate cortex were ablated(Zheng et al., 2020). Lesions within the MD are also associated with impaired fear extinction(Lee et al., 2011), and injecting gabazine, a modulator of extra-synaptic GABA receptors, into the MD facilitated extinction(Paydar et al., 2014).

Evidence regarding the involvement of the thalamus in the context of threat learning in humans is relatively sparse. Much of our knowledge comes from studies focusing on attention, perception, and decision-making. For example, the LGN has been mainly viewed as a transmitter of peripheral information to other brain regions and found to be associated with selective attention and anticipation of visual stimuli(Mahoney and Schmidt, 2024; O'Connor et al., 2002; Saalmann and Kastner, 2009). The MD contribution to perception, spatial attention, and decision-making has also been reported(Griffiths et al., 2022; Wurtz et al., 2011). Beyond cognitive research, some human studies have specifically investigated the pulvinar's engagement in threat detection. Individuals with increased fiber density in the pulvinar-amygdala pathway showed an enhanced ability to recognize fearful faces(McFadyen et al., 2019). A patient with a complete lesion in the left pulvinar showed slower responses to threatening images when stimuli were presented on the ipsilesional, but not contralesional, field(Ward et al., 2005). In agreement with this, unseen stimuli (fearful vs. happy faces) presented on the blind side of patients with hemianopia moderated their performance when the pulvinar was spared but not when it was lesioned(Bertini et al., 2018).

Specific thalamic contribution to threat processing is still largely unknown, and translational research on this topic is limited. We aim to address these critical gaps in our understanding by investigating the distinct neural representations of associative threat learning in the human pulvinar divisions, LGN, and MD. We analyzed the neuroimaging data of 293-412 controls. All participants underwent a two-day threat learning paradigm(Milad et al., 2009, 2007; Wen et al., 2024, 2022) while in the fMRI scanner. The conditioned stimulus (CS+) (e.g., red light) was associated with an electric shock (unconditioned stimulus US, 62.5% reinforcement rate), while a control light (e.g., blue) was never paired with the US (CS-). This conditioning phase occurred in a computer-displayed visual context A (e.g., an office). The extinction learning included presenting the CS+ and CS- with no US reinforcement in a distinct context B (e.g., bookcase). In extinction recall and threat renewal, the extinguished stimuli were presented with no US reinforcement within contexts B (safe contextual cues) and A (threat contextual cues), respectively. Schematic illustrations of each phase of the paradigm are presented in **Figs.** 1a, 4a-6a.

We focus on neural activation patterns within pulvinar divisions, LGN, and MD while acquiring the CS-US association. As associative learning is a rapid psychological process(Konrad et al., 2024), we analyzed the first four trials of all threat learning phases. We compared brain activation (BOLD) to the CS+ vs. CS- at the block level by averaging the activation across all four trials and at a trial-by-trial level to provide finer activation temporal resolution. This dual approach allows us to capture the general neural responses associated with associative threat learning and provides new insights into trial-

level dynamics(Wen et al., 2022). The current dominant neurocognitive thalamic models(Sherman, 2007; Sherman and Guillery, 2006) highlight the thalamus's role in mediating cortical-cortical communications and facilitating high-order functions. Based on this view, we anticipate distinct pulvinar, MD, and LGN roles. The LGN, as a first-order nucleus, is expected to serve relay functions, transmitting information with minimal integrations. The pulvinar and MD, on the other hand, as higher-order nuclei, are likely involved in more complex processing, potentially integrating threat-related information.

Results

Parallel functional representation of associative threat learning in the anterior pulvinar and MD during conditioning

The anterior pulvinar and MD contribute to early associative threat learning, as evidenced by increased functional activation in response to CS+ compared to CS- at the block level (**Fig.** 1b-c). The trial-wise analysis revealed a distinct activation pattern. In the first trial, we observed similar activation levels for both CS+ and CS- (no significant difference), but in the subsequent trial, the BOLD signal in both regions was heightened specifically for CS+ (**Fig.** 1b-c, Extended Tables 1-2). In our paradigm, the electric shock was paired with CS+ at the end of the CS presentation. The similarity in BOLD responses to CS+ and CS- during the first trial likely reflects an initial equivalence in the emotional valence of the stimuli. The gradual increase in activation for CS+ by the second trial suggests a shift in the emotional valence, indicating rapid associative learning.

166 The similarity in trial-level activation patterns in the anterior pulvinar and MD raises the
167 question of whether this apparent similarity truly reflects a parallel functional contribution
168 to associative threat learning. To test this possibility, we first quantified the trial-wise
169 relationships using Pearson correlation coefficients between the two regions. The
170 observed correlations support consistent co-activation across all corresponding trials (r
171 values ≥ 0.66, $p < 0.001$, **Fig.** 2a, left). However, this approach could not exclude the
172 possibility that the shared variance is a consequence of shared anatomical proximity,
173 particularly because both regions are part of the same brain structure, i.e., the thalamus.
174 To control for this confound, we conducted a hierarchical regression model in four steps
175 for each trial. We modeled MD activation as the target and progressively added the
176 pulvinar divisions as covariates. Despite small variations in regression weights (beta
177 values) across control models, the anterior pulvinar consistently exhibited the highest
178 beta estimates (**Fig.** 2a, middle). Importantly, these values remain consistent across
179 10,000 bootstrapping iterations with replacements, suggesting that the anterior pulvinar
180 effect is robust and stable across resampled datasets (**Fig.** 2a, right). Additionally, the
181 anterior pulvinar explained the largest proportion of variance in MD activation (r^2 = 43-
182 60.7%) relative to other pulvinar divisions, which negligibly contributed to this parameter
183 (pie charts, **Fig.** 2a). Finally, applying the same analytical approach while controlling for
184 the LGN activation as an alternative anatomical control beyond the pulvinar itself, yielded
185 similar results (**Fig.** 2b). Together, these analyses support preferential trial-wise functional
186 co-activations between the anterior pulvinar and MD, independent of shared anatomical
187 proximity.
188

Although co-activation does not necessarily imply similar activation magnitude, we further tested the differences in activation levels in the anterior pulvinar and MD. We used a t-test to capture the differences in the overall activation at the block level and repeated measures analysis of variance (RM-ANOVA) to capture the activation differences at the trial level. The results showed that the overall MD activation in response to CS+ was higher than the anterior pulvinar response (p-value < 0.001, **Fig.** 2c). The trial-wise analysis revealed heightened activation in the MD compared to the anterior pulvinar, particularly during trials 3 and 4 (p_{FDR}-values < 0.05, **Fig.** 2c). The increased activation within the MD potentially reflects its role in deeper processing of threat relatively to the anterior pulvinar.

A data-driven approach reveals hierarchical functional processing of threat in pulvinar divisions

The anatomical and functional interconnections between pulvinar divisions remain insufficiently characterized. To address this gap and understand the pulvinar's role in early associative threat learning, we integrated findings from complementary analyses into a novel model designed to investigate the functional relationships between pulvinar divisions.

We first defined the activation within each pulvinar division as the differences in BOLD signal at the block level in response to CS+ compared to CS-. We then performed RM-ANOVA to test whether the pulvinar divisions were engaged with different activation levels. We found no activation differences, suggesting similar processing levels of CS+

212 information across all pulvinar divisions (**Fig.** 3a). Using network analysis, we explored
213 the underlying functional dynamics between the divisions. We employed the EBICglasso
214 method(Foygel and Drton, 2010) to estimate a sparse Gaussian graphical model. To
215 assess the stability of the network and provide robust estimates of edges and centrality
216 measures, we conducted 10,000 bootstrap resamples. This approach allowed us to
217 compute 95% confidence intervals, ensuring the reliability of our findings. The combined
218 use of EBICglasso and bootstrapping is essential for accurately capturing the dynamics
219 of pulvinar division interactions. The resulting network included four nodes and five edges.
220 The network plot pointed to stable direct edges connecting the lateral pulvinar to the
221 anterior pulvinar and indirect edges connecting both the lateral and inferior pulvinar to the
222 anterior through the medial pulvinar (**Fig.** 3b). Additionally, the medial pulvinar exhibited
223 the highest centrality values, a measure that captures the node importance within a
224 network, indicating a potential hub role of this division in associative threat learning (**Fig.**
225 3b).

226 These underlying dynamics and the activation timing in the trial-wise analyses (overview
227 in **Fig.** 3c and details in **Fig.** 1b) led us to propose a functional model of the relationships
228 between pulvinar divisions. Specifically, the increased activation induced by CS+ during
229 trial 1 in the medial, inferior, and lateral pulvinar suggests that these divisions process
230 CS+ information before the anterior pulvinar, which exhibited a delayed BOLD response
231 starting in trial 2. The medial pulvinar mediates connections within the pulvinar network
232 and is associated with elevated centrality values. Together, these findings highlight the
233 hub role of the medial pulvinar, integrating CS+ information at a higher level, compared
234 to sensory-driven processing in the inferior and lateral pulvinar. This possible hierarchical

organization is supported by previous evidence showing that the inferior and lateral pulvinar are associated with processing basic sensory information(Berman and Wurtz, 2010, 2008; Cortes et al., 2024), while the medial pulvinar is implicated in higher-order processing, including attention and working memory(Homman-Ludiye and Bourne, 2019) (**Fig.** 3d).

This data-driven approach provides a new perspective on the pulvinar divisions' functional specialization during associative threat learning. We hypothesize that, during this process, the activation in the medial pulvinar mediates the functional relationships between the inferior and lateral divisions with the anterior pulvinar (**Fig.** 3e). To test this, we conducted a mediation model analysis and evaluated the model robustness using the k-fold cross-validation method. The sample (N = 293) was randomly divided into three groups of 91, 96, and 106 subjects. Each sub-sample was used to test the model while the remaining groups served as a training phase. This resulted in six iterations of the mediation model. The 95% Confidence Intervals for each path coefficient were estimated using 10,000 bootstrapping replications. This choice was made to achieve greater precision and stability in the confidence interval estimates. Finally, applying the mediation analysis to another independent cohort (N = 114) confirmed the model's applicability. The results in **Figs.** 3f-3g support the mediating role of the medial pulvinar, demonstrating significant indirect paths from the lateral and inferior divisions to the anterior pulvinar. Detailed parameters are presented in Extended Table 3.

Pulvinar divisions and MD support extinction learning while preserving threat memory across contextual cues

257 After our comprehensive examination of the thalamic contribution to threat conditioning,
258 we moved forward to examine the neural contributions of the same regions to extinction
259 learning. During this phase, we found higher activation in response to CS+ than CS-
260 across all pulvinar divisions and MD at the block level. The trial-wise analysis
261 demonstrated that these differences are mainly driven by the first two trials (**Figs.** 4b and
262 4c). Together, the pulvinar divisions and MD showed a similar activation pattern where
263 the BOLD signal induced by the CS+ is significantly diminished after trial 2, highlighting
264 these nuclei's engagement in rapid extinction learning. Detailed parameters are
265 presented in Extended Tables 4-5.
266
267 During extinction recall, the anterior pulvinar and MD exhibited similar functional patterns
268 at both block and trial levels, with increased activation to CS+ compared to CS- during
269 the first two trials. In contrast, the medial and inferior pulvinar maintained the BOLD signal
270 to CS+ in the second trial while showing reduced responses to CS-. We observed no
271 activation differences in the lateral pulvinar (**Fig.** 5b-c, Extended Tables 6-7). This finding
272 highlights the involvement of most pulvinar divisions and MD in sustaining threat memory
273 under safe contextual cues and suggests retrieval suppression of the extinguished threat.
274
275 Changing the contextual cues to a threat background where the original associative
276 learning occurred elicited increased activation in response to CS+ in the anterior, inferior,
277 and lateral pulvinar divisions along with the MD (**Fig.** 6b-c, Extended Tables 8-9). These
278 regions are, therefore, involved in the reactivation of threat memory, a hallmark process
279 in the threat renewal phase.

280

281 **Consistent LGN activation patterns across all threat learning phases align with**
282 **principles of feedforward processing.**

283 At the block level, we observed elevated activation in response to CS+ compared to CS-
284 across conditioning, extinction, recall, and renewal. These differences were driven by the
285 first trial, during which an increased BOLD signal in response to CS+ was followed by a
286 decline in subsequent trials (**Figs.** 1d, 4d-6d, Extended Tables 2, 5, 7, and 9). These
287 findings suggest that the LGN plays a consistent role across different phases of threat
288 learning, potentially reflecting early attentional processing or anticipation of upcoming
289 visual stimuli.

290

291 **Thalamic connectivity underlies threat learning and memory**

292 We tested the relationships between each thalamic nucleus and core brain regions within
293 the 'fear circuit'(Herry et al., 2010; Maren and Quirk, 2004; Milad et al., 2014; Milad and
294 Quirk, 2012; Tovote et al., 2015) by seeding the nuclei to target the amygdala,
295 hippocampus, ventromedial prefrontal cortex (vmPFC), subgenual anterior cingulate
296 cortex (sgACC), and dorsal anterior cingulate cortex (dACC). During conditioning, the
297 anterior pulvinar exhibited positive connectivity with the amygdala, vmPFC, and
298 hippocampus (all $p_{FDR} < 0.05$ and all 95% bias-corrected and accelerated (BCa)
299 confidence intervals (CI) of the mean differences from 10,000 bootstrap resamples
300 excluded zero; Cohen's ds = 0.14, 0.14, and 0.15, with corresponding 95% parametric
301 CIs also excluding zero) (**Fig.** 1e). The connectivity with the amygdala likely supports
302 encoding the emotional valence of the newly learned CS-US associations, while the

engagement of the hippocampus suggests prioritizing the contextual CS+ information. The connectivity with the vmPFC may underlie a process of top-down control release to enhance fear expression or encode threat information for tracking and supporting decision-making in future encounters.

During extinction learning, we found increased LGN-sgACC connectivity ($p_{FDR} < 0.05$ and 95% BCa CIs of the mean differences from 10,000 bootstrap resamples excluded zero; Cohen's d = 0.15, 95% parametric CI [0.035, 0.256]), suggesting sgACC involvement in emotional regulation (**Fig.** 4e). Interestingly, in recall and renewal, we found that the learners, i.e., the anterior pulvinar and MD contribute to supporting either safe or threatening memory, depending on contextual cues. Specifically, the MD-dACC connectivity supported safe memory in recall ($p_{FDR} < 0.05$ and 95% BCa CI of the mean differences from 10,000 bootstrap resamples excluded zero; Cohen's d = 0.13, 95% parametric CI [0.031, 0.225]; **Fig.** 5e), whereas anterior pulvinar-vmPFC supported threatening memory in renewal ($p_{FDR} < 0.01$ and 95% BCa CI of the mean differences from 10,000 bootstrap resamples excluded zero; Cohen's d = 0.20, 95% parametric CI [0.084, 0.306]; **Fig.** 6e).

Discussion

We examined the neural representation of associative threat learning within the pulvinar divisions, LGN, and MD, providing new insights into thalamic involvement in this adaptive behavior in humans. We identified distinct roles among these thalamic nuclei with respect to their activation profiles during threat learning and memory. The anterior pulvinar and MD exhibited parallel activation patterns consistent with associative learning, reflecting

325 their roles in automatic survival responses and deliberate threat processing. We propose
326 a novel hierarchical model for processing threat information in the pulvinar divisions. The
327 medial pulvinar mediates basic sensory information from the inferior and lateral divisions
328 to the anterior pulvinar for higher-order integrative learning. Both pulvinar and MD were
329 involved in extinction and showed activation consistent with the salience processing of
330 threat-related memories during extinction recall and threat renewal. The LGN primarily
331 represented feedforward processing, anticipating upcoming visual stimuli throughout all
332 phases of threat learning. We integrated these insights into schematic models underlying
333 the emotional and behavioral expression of threat learning and memory, providing a
334 neural framework for studying related human behaviors (**Fig.** 7a-b).

335 The anterior pulvinar and MD co-activation patterns demonstrate a parallel contribution
336 to threat learning. The similar activation in response to CS+ and CS- at the first trial,
337 followed by a heightened activation specific to CS+ in the next trial, is consistent with the
338 acquisition of the CS-US association. The responses' similarity to both types of CS during
339 the first trial suggests an equivalent initial emotional valence. The gradual increase in the
340 activation, specifically to CS+ by the end of trial 1, suggests a shift in the emotional
341 valence of CS+, indicating rapid associative learning. This parallel specialized role
342 highlights the anterior pulvinar and MD as central thalamic hubs for integrating CS-US
343 information, specifying the two-system model proposed by LeDoux and Pine(LeDoux and
344 Pine, 2016). Briefly, fear processing, according to this model, involves two distinct
345 pathways: a subcortical route for rapid threat detection and species-specific defense
346 reactions and a cortical route for deliberate threat evaluation and conscious fear
347 experience. Learning within the anterior pulvinar appears to support rapid automatic

348 processes of the subcortical pathway. This aligns with previous reports that demonstrated
349 the role of the pulvinar-amygdala pathway in encoding negative emotions in
350 humans(Bridge et al., 2015; Koller et al., 2019; Kragel et al., 2021; McFadyen et al., 2019;
351 Rafal et al., 2015). Indeed, the increased connectivity that we observed with the
352 amygdala, hippocampus, and vmPFC during threat conditioning aligns with this role.
353 Specifically, in this context, the amygdala likely contributes to tagging a negative
354 emotional valence to CS+ and triggering fight, flight, or freeze reactions(Adolphs et al.,
355 1994; Costa et al., 2022; Fanselow and LeDoux, 1999; Phelps and LeDoux, 2005; Wen
356 et al., 2024, 2022). The connectivity with the hippocampus likely facilitates contextual
357 encoding of the environmental characteristics of the aversive event(Maren, 2001; Maren
358 et al., 2013). In turn, the connectivity with vmPFC appears to support salience encoding
359 for tracking future encounters with the learned threat(Battaglia et al., 2020) and facilitating
360 decision-making and emotion regulation(Milad and Quirk, 2012, 2002; Nejati et al., 2021).

361 On the other hand, MD activation aligns more closely with the cortical pathway, facilitating
362 conscious and deliberate threat encoding. This is supported by our findings, which
363 showed increased MD activation in response to CS+, compared to the anterior pulvinar
364 during threat learning, indicating a broader or deeper processing of the CS-US
365 association. Additionally, this interpretation is supported by substantial evidence pointing
366 to well-established anatomical pathways connecting the MD with the PFC and
367 demonstrating its role in decision-making and learning(Behrens et al., 2003; Hwang et
368 al., 2020; Li et al., 2022; Wolff and Halassa, 2024). This is along with reports that
369 underscored the contribution of the MD-cortical loops to supporting a conscious
370 experience in humans(Griffiths et al., 2022; Whyte et al., 2024). Together, these findings

371 advance our understanding of the two-system model of threat processing, highlighting the
372 anterior pulvinar and MD role in the acquisition of the CS-US association and suggesting
373 that these regions underlie a parallel conscious vs. unconscious learning proposed by
374 LeDoux and colleagues(LeDoux and Pine, 2016), **Fig.** 7a.

375 Our findings demonstrate that different pulvinar divisions hierarchically contribute to the
376 integration of CS-US association in the anterior pulvinar through bottom-up processing.
377 Although the anatomical projections within pulvinar divisions are not well characterized,
378 our functional data-driven approach revealed a critical role for the medial pulvinar as a
379 hub region facilitating communication among pulvinar divisions. Specifically, our trial-wise
380 analysis showed that the medial, inferior, and lateral pulvinar process threat-related
381 information earlier than the anterior pulvinar. The anterior pulvinar exhibited activation in
382 response to CS+ starting at trial 2, whereas activation in the other pulvinar divisions
383 occurred as early as trial 1. Network modeling further identified the medial pulvinar as a
384 central hub, facilitating communication with other divisions. Using a robust mediation
385 model, we demonstrated that the medial pulvinar appears to mediate the relay of sensory
386 CS+ information from the inferior and lateral pulvinar to the anterior division for higher-
387 order integrative learning. This hierarchical model aligns with previous evidence
388 suggesting that the inferior and lateral pulvinar are associated with processing basic
389 sensory information(Berman and Wurtz, 2010, 2008; Bridge et al., 2015; Cortes et al.,
390 2024). While the medial pulvinar, which receives projections from deep layers of the
391 superior colliculus, supports more advanced functions such as attention and working
392 memory(Bridge et al., 2015; Homman-Ludiye and Bourne, 2019). These findings provide
393 novel insights into the functional specialization of pulvinar divisions during threat learning,

394 suggesting feedforward functions in the inferior and lateral pulvinar and high-order
395 integration in the anterior pulvinar.

396 The pulvinar divisions and MD are actively engaged in extinction learning, as indicated
397 by increased activation in response to CS+ during the first two trials, followed by a
398 diminished response. This decline in activation likely reflects a shift in the emotional
399 valence of the CS+ to match that of the CS-, suggesting a rapid extinction process in the
400 human thalamus. Despite the involvement in extinction, these nuclei remained sensitive
401 to the extinguished threat during safe contextual cues in extinction recall and exhibited
402 increased activation to the extinguished CS+ when the stimuli were presented within
403 threat contextual cues during renewal. This pattern suggests engagement in retrieval
404 suppression during recall, along with threat salience processing during both recall and
405 renewal. The MD and pulvinar continue to monitor and evaluate the extinguished threat
406 across contexts rather than relying on static safety memories. These nuclei appear to
407 engage in dynamic evaluation, learning, and decision-making during future encounters
408 with the extinguished CS+.

409 The classical Pavlovian model proposes that extinction learning forms a new safety
410 memory, competing with the original threat memory acquired during conditioning(Bouton,
411 2002; Milad and Quirk, 2002). Contextual changes often favor either the safe or threat
412 memory. Maren and colleagues(Maren et al., 2013; Maren and Quirk, 2004) described
413 the hippocampal-prefrontal-amygdala model for contextual memory. The hippocampus
414 projects to the basolateral amygdala, vmPFC, and dACC. Although the vmPFC supports
415 safe memory recall by projecting to the intercalated cells (which inhibit the central nucleus

416 of the amygdala), the dACC enhances threat memory renewal by projecting to the
417 basolateral amygdala (which activates the central nucleus of this structure). Our findings
418 suggest that the thalamic connectivity may influence the balance between recalling safe
419 vs. threat memory by modulating the competitive interaction between the dACC and
420 vmPFC. The increased MD-dACC connectivity during recall may reflect a thalamic-driven
421 reconfiguration of prefrontal circuits, enabling the vmPFC to become more functionally
422 dominant and promote safe memory expression. On the other hand, the anterior pulvinar-
423 vmPFC connectivity during renewal may destabilize the influence of the vmPFC, allowing
424 the dACC to regain dominance and facilitate threat memory retrieval. The thalamic
425 connectivity, thus, appears to orchestrate a context-dependent functional balance
426 between the dACC and vmPFC. This balance may serve as a neural "toggle switch"
427 between safe vs. threat memory expression. We integrated this suggested flexible
428 responding mechanism to changing environmental contexts in Maren's circuit model of
429 emotional memory, **Fig.** 7b.

430 The LGN contribution is consistent across all phases of threat learning, as evidenced by
431 our trial-wise results, which pointed to increased activation in response to CS+ that
432 diminished immediately after the first trial. This distinct pattern indicates readiness for
433 imminent visual stimuli, regardless of the actual emotional valence, as conditioning,
434 extinction, recall, and renewal elicited similar BOLD patterns. This aligns with previous
435 studies that highlighted the LGN's engagement in selective attention and anticipation of
436 visual stimuli(Mahoney and Schmidt, 2024; O'Connor et al., 2002; Saalmann and
437 Kastner, 2009). The LGN, as a first-order nucleus(Cortes et al., 2024), primarily supports
438 a feedforward function, while the pulvinar, as part of the visual thalamus, is more closely

associated with a broader functional processing(Cortes et al., 2024) including emotional valences of stimuli. This distinction underscores their joint but specialized contributions to adaptive threat responses.

Although distinct thalamic roles in threat learning have been proposed, fMRI data do not fully capture the complexity of this structure. Pulvinar divisions, MD, and LGN each contain different neuron subtypes and finer anatomical subdivisions, which may serve diverse functions. Future advancements, such as higher-resolution human brain atlases, could improve our ability to study these nuclei with better anatomical precision. Additionally, since different sensory modalities preferentially engage distinct thalamic nuclei, the specific thalamic roles we described may not be consistent across different experimental designs, particularly in studies using auditory threat learning. The pulvinar divisions' relationships during conditioning are purely functional and might be supported by direct or indirect anatomical projections. Finally, given the indirect nature of fMRI data and the absence of direct brain signal manipulations, our findings should not be interpreted as evidence of causality. Further research is needed to examine causal mechanisms underlying dynamic neural representations of threat learning within the thalamus.

This study's insights raise critical future questions at the intersection between neuroscience, psychology, and mental health, particularly regarding the neural mechanisms underlying associative threat learning. First, the crucial role of the anterior pulvinar and MD during the acquisition of the CS-US association sets the stage for developing more precise brain interventions, focusing on refining maladaptive fear

461 reactions. Future studies could explore the optimal parameters for applying non-invasive
462 techniques to inhibit these thalamic regions during or immediately after fear conditioning.
463 This approach is particularly promising for clinical populations and individuals exposed to
464 high-risk environments, such as emergency medical staff, firefighters, and paramedics.

465 Second, the distinct contributions of the MD-dACC and anterior pulvinar-vmPFC circuits
466 to safe vs. threatening memory suggest potential intervention targets for prioritizing one
467 memory over the other. Activating the MD-dACC may facilitate recalling safe memories
468 while engaging the anterior pulvinar-vmPFC circuits might reinforce fear memory
469 pathways. Experimental designs in controlled laboratory settings could target these
470 circuits to identify specific parameters for enhancing safe memories. This avenue holds
471 therapeutic potential, particularly in conditions such as aviophobia; activating a safe
472 memory circuit before a flight might suppress fear relapse during the actual flight.

473 Third, the anterior pulvinar-MD relationships raise questions related to the wide range of
474 human behaviors, focusing on understanding neural gateways between conscious and
475 unconscious learning. Studying the dynamics of information flow across this promising
476 pathway could deepen our understanding of how sensory and cognitive information
477 transits between conscious and unconscious states and brings about behaviors. This
478 research line may pave the way for innovative learning methods and reveal
479 neurocognitive mechanisms underlying the acquisition of new information in humans.

480 Together, our findings and emerging research directions underscore the thalamic nuclei's
481 vital role as a hub for fear acquisition and memory processing, offering promising avenues
482 for theoretical advancements and clinical applications. As the primary neural gateway to

483 the human brain, the thalamus is the first station for all sensory information except
484 olfactory inputs. Modulating its functions is potentially an impactful strategy to induce
485 widespread functional changes across the brain and influence different mental and
486 behavioral expressions.

487 **Materials and Methods**

488 **Participants**

489 We analyzed the fMRI data of 293-412 human subjects of both sexes, aged 18-70 years
490 old (M = 32.17 ± 13.1). All participants were proficient in English, right-handed, and had
491 normal or corrected-to-normal vision. The exclusion criteria included a history of seizures
492 or significant head trauma, current substance abuse or dependence, metal implants,
493 pregnancy, breastfeeding, or positive urine toxicology screen for drugs of abuse. We
494 followed the latest version of Helsinki's declaration, and all procedures were approved by
495 the Partners HealthCare Institute Review Board of the Massachusetts General Hospital,
496 Harvard Medical School. All subjects provided written informed consent before taking part
497 in the study. Results from this dataset have been published elsewhere with a different
498 focus(Marin et al., 2020; Wen et al., 2024, 2022). The current results are novel and have
499 not been previously published.

500

501 **Experimental procedure**

502

503 Participants underwent two-day sessions of a validated threat learning paradigm in the
504 MRI scanner (**Figs.** 1a, 4a-6a); the experimental contexts consisted of visual scenes on
505 a computer display. On day 1, participants underwent a Pavlovian conditioning phase in
506 which a neutral stimulus in context A (e.g., red light in an office) was paired with a 500ms

electric shock (US) with a partial reinforcement rate of 62.5%. Another neutral stimulus in context A (e.g., blue light in the same office) was also presented but never paired with the shock (CS-). Participants were guided to select a highly annoying but nonpainful shock level during a pre-experiment calibration stage, and we used that personalized level during conditioning. On the same day, we also conducted extinction learning in context B (e.g., red and blue lights in a casebook background). The stimuli were repeatedly presented with the removal of the expected reinforcement (i.e., no shock).

On day 2, the participants underwent two phases of a memory test. The first is extinction recall, including presenting the extinguished CS+ and CS- within safe contextual cues (context B used during extinction learning). The second is threat renewal, in which the stimuli were presented within threat contextual cues (context A used in conditioning). Both extinction recall and threat renewal included no US reinforcement. Across phases of threat learning, the duration of each trial was 6s, and the inter-trial intervals with a fixation screen ranged between 12 to 18 s (15 s on average). Finally, to control for potential confounds related to the experimental design, we pseudorandomized and counterbalanced the order of CS+ and CS− across phases and between subjects.

MRI data acquisition and preprocessing

Two MRI settings were used to acquire the neuroimaging data. The first is a Trio 3T whole-body MRI scanner (Siemens Medical Systems, Iselin, New Jersey) using an 8-channel head coil. The functional data in this setting were acquired using a T2* weighted echo-planar pulse sequence with these parameters: TR = 3.0s, TE = 30 ms, slice number = 45,

530 voxel size = 3 × 3 × 3 mm^3. The second setting was also in the same scanner using a 32-
531 channel head coil. The functional images were obtained using a T2* weighted echo-planar
532 pulse sequence using TR = 2.56s TE = 30 ms, slice number = 48, voxel
533 size = 3 × 3 × 3 mm^3. The anatomical brain images were collected using a T1-weighted
534 MP-RAGE pulse sequence, parcellated into 1 × 1 × 1 mm^3 voxels. Elastic bands were
535 affixed to the head coil device to reduce head motions.
536
537 Using the default pipeline in fMRIPrep, version 20.0.2(Esteban et al., 2020, 2019), we
538 preprocessed the data and applied correction of slice timing, realignment of the functional
539 images, and coregistration. In addition, the data was normalized into the Montreal
540 Neurological Institute (MNI) space and smoothed with a 6-mm full-width half-maximum
541 Gaussian kernel.
542
543 **Activation analyses**
544 We applied the least-squares-based generalized linear model (GLM) for each participant
545 to estimate the BOLD response to CS+ and CS- using SPM 12. We estimated the beta
546 values for each voxel during each learning phase in the paradigm. Overall, the model
547 included 32 regressors for the CS+ and CS-, a regressor for the context, and a regressor
548 for shock in conditioning but not in other phases. The GLM also included six head
549 movement parameters (x, y, z directions, and rotations). This first-level analysis resulted
550 in contrast maps that we used to estimate the variability of these maps across all subjects
551 at the group-level analysis. We then used the contrast maps from the group-level analysis
552 to extract the averaged values across the voxels within predefined masks of the pulvinar

553 divisions, MD, and LGN. These outputs were used to compare the BOLD response during
554 the first four CS+ and four CS- trials. We averaged the activation for each CS type across
555 trials to obtain the block-level activation.
556
557 The statistical analyses included t-tests, RM-ANOVA, network analyses, mediation
558 models, and hierarchical regression models. All were conducted using JASP versions
559 0.18.3 and 0.19.3(JASP Team, 2024). False discovery rate (FDR) correction was applied
560 across analyses. RM-ANOVA was used to analyze trial-by-trial BOLD responses as the
561 same participants were measured across the trials. Assumptions of sphericity were
562 checked, and Greenhouse-Geisser corrections were applied where necessary.
563
564 **Connectivity analyses**
565 We computed the connectivity values using the CONN functional connectivity toolbox,
566 version 22. a, for the MathWorks MATLAB program(Nieto-Castanon and Whitfield-
567 Gabrieli, 2022; Whitfield-Gabrieli and Nieto-Castanon, 2012). We first segmented the
568 brain images into different tissues of gray matter, white matter, and CSF. Then, we applied
569 the standard denoising pipeline in the CONN toolbox(Nieto-Castanon, 2020) to the
570 functional images to control the effect of potential confounding parameters, using a
571 component-based noise correction method. Finally, bandpass frequency filtering of the
572 BOLD time series between 0.008 Hz and 0.09 Hz was also applied.

573 We evaluated differences in connectivity between CS+ and CS− conditions using
574 generalized psychophysiological interaction (gPPI) analyses. We defined the first eight
575 trials of each condition as a block. The pulvinar divisions, MD, and LGN were defined as

576 individual seed regions, and connectivity was assessed with target regions, including the
577 dACC, sgACC, vmPFC, amygdala, and hippocampus. The model included seed BOLD
578 signals as physiological factors, boxcar signals characterizing the task conditions
579 convolved with an SPM canonical hemodynamic response function as psychological
580 factors, and the product of the two as psychophysiological interaction terms. Functional
581 connectivity changes were quantified using Fisher-transformed correlation coefficients of
582 the psychophysiological interaction terms. At the group level, we used a GLM to assess
583 task-related connectivity changes across participants. Differences in connectivity
584 between conditions were evaluated using paired t-tests, applying false discovery rate
585 (FDR) correction at $p < 0.05$. 10,000 bootstrap resamples were used to obtain BCa CI,
586 providing more robust estimates of the connectivity mean differences.

587 **Masks**

588 We defined the pulvinar divisions, MD, and LGN nuclei using predefined masks based on
589 the neuroanatomical guidelines of the Automated Anatomical Labelling Atlas(Rolls et al.,
590 2020). We also applied the same atlas guidelines to determine the masks for the two
591 other anatomical regions; the amygdala and hippocampus. The masks for the functional
592 regions were created using Neurosynth(Yarkoni et al., 2011) and the keyword
593 'conditioning.' For each region, we created 8mm spheres around the following identified
594 peak coordinates: vmPFC (MNIxyz = −2, 46, −10), sgACC (MNIxyz = 0, 26, −12), and
595 dACC (MNIxyz = 0, 14, 28).
596
597

Acknowledgments

This work was supported by the National Institute of Mental Health grants R01MH123736, R01MH125198, R33MH111907, R01MH097880, and R01MH097964 to M.R.M.

References

Adolphs R, Tranel D, Damasio H, Damasio A. 1994. Impaired recognition of emotion in facial expressions following bilateral damage to the human amygdala. *Nature 1994 372:6507* **372**:669–672. doi:10.1038/372669a0

Arcaro MJ, Pinsk MA, Kastner S. 2015. The Anatomical and Functional Organization of the Human Visual Pulvinar. *Journal of Neuroscience* **35**:9848–9871. doi:10.1523/JNEUROSCI.1575-14.2015

Badarnee M, Wen Z, Hammoud MZ, Glimcher P, Cain CK, Milad MR. 2025. Intersect between brain mechanisms of conditioned threat, active avoidance, and reward. *Communications Psychology* **3**:32. doi:10.1038/S44271-025-00197-7

Battaglia S, Garofalo S, di Pellegrino G, Starita F. 2020. Revaluing the Role of vmPFC in the Acquisition of Pavlovian Threat Conditioning in Humans. *Journal of Neuroscience* **40**:8491–8500. doi:10.1523/JNEUROSCI.0304-20.2020

Behrens TEJ, Johansen-Berg H, Woolrich MW, Smith SM, Wheeler-Kingshott CAM, Boulby PA, Barker GJ, Sillery EL, Sheehan K, Ciccarelli O, Thompson AJ, Brady JM, Matthews PM. 2003. Non-invasive mapping of connections between human thalamus and cortex using diffusion imaging. *Nat Neurosci* **6**:750–757. doi:10.1038/NN1075;KWRD=BIOMEDICINE

Berman RA, Wurtz RH. 2010. Functional Identification of a Pulvinar Path from Superior Colliculus to Cortical Area MT. *Journal of Neuroscience* **30**:6342–6354. doi:10.1523/JNEUROSCI.6176-09.2010

Berman RA, Wurtz RH. 2008. EXPLORING THE PULVINAR PATH TO VISUAL CORTEX. *Prog Brain Res* **171**:467. doi:10.1016/S0079-6123(08)00668-7

Bertini C, Pietrelli M, Braghittoni D, Làdavas E. 2018. Pulvinar lesions disrupt fear-related implicit visual processing in hemianopic patients. *Front Psychol* **9**:412050. doi:10.3389/FPSYG.2018.02329/BIBTEX

Bouton ME. 2002. Context, ambiguity, and unlearning: Sources of relapse after behavioral extinction. *Biol Psychiatry* **52**:976–986. doi:10.1016/S0006-3223(02)01546-9

Bridge H, Leopold DA, Bourne JA. 2015. Adaptive pulvinar circuitry supports visual cognition. *Trends Cogn Sci* **20**:146. doi:10.1016/J.TICS.2015.10.003

Carr JA. 2015. I'll take the low road: The evolutionary underpinnings of visually triggered fear. *Front Neurosci* **9**:165437. doi:10.3389/FNINS.2015.00414/BIBTEX

Casanova C, Chalupa LM. 2023. The dorsal lateral geniculate nucleus and the pulvinar as essential partners for visual cortical functions. *Front Neurosci* **17**:1258393. doi:10.3389/FNINS.2023.1258393/BIBTEX

Cortes N, Ladret HJ, Abbas-Farishta R, Casanova C. 2024. The pulvinar as a hub of visual processing and cortical integration. *Trends Neurosci* **47**:120–134. doi:10.1016/J.TINS.2023.11.008

Costa M, Lozano-Soldevilla D, Gil-Nagel A, Toledano R, Oehrn CR, Kunz L, Yebra M, Mendez-Bertolo C, Stieglitz L, Sarnthein J, Axmacher N, Moratti S, Strange BA. 2022. Aversive memory formation in humans involves an amygdala-hippocampus phase code. *Nature Communications 2022 13:1* **13**:1–16. doi:10.1038/s41467-022-33828-2

683 Esteban O, Ciric R, Finc K, Blair RW, Markiewicz CJ, Moodie CA, Kent JD, Goncalves
684 M, DuPre E, Gomez DEP, Ye Z, Salo T, Valabregue R, Amlien IK, Liem F, Jacoby N,
685 Stojić H, Cieslak M, Urchs S, Halchenko YO, Ghosh SS, De La Vega A, Yarkoni T,
686 Wright J, Thompson WH, Poldrack RA, Gorgolewski KJ. 2020. Analysis of task-
687 based functional MRI data preprocessed with fMRIPrep. *Nat Protoc* **15**:2186–2202.
688 doi:10.1038/S41596-020-0327-3
689 Esteban O, Markiewicz CJ, Blair RW, Moodie CA, Isik AI, Erramuzpe A, Kent JD,
690 Goncalves M, DuPre E, Snyder M, Oya H, Ghosh SS, Wright J, Durnez J, Poldrack
691 RA, Gorgolewski KJ. 2019. fMRIPrep: a robust preprocessing pipeline for functional
692 MRI. *Nat Methods* **16**:111–116. doi:10.1038/S41592-018-0235-4
693 Fanselow MS, LeDoux JE. 1999. Why we think plasticity underlying pavlovian fear
694 conditioning occurs in the basolateral amygdala. *Neuron* **23**:229–232.
695 doi:10.1016/S0896-6273(00)80775-8
696 Foygel R, Drton M. 2010. Extended Bayesian Information Criteria for Gaussian
697 Graphical Models. *Adv Neural Inf Process Syst* **23**.
698 Fullana MA, Harrison BJ, Soriano-Mas C, Vervliet B, Cardoner N, Àvila-Parcet A, Radua
699 J. 2015. Neural signatures of human fear conditioning: an updated and extended
700 meta-analysis of fMRI studies. *Molecular Psychiatry 2016 21:4* **21**:500–508.
701 doi:10.1038/mp.2015.88
702 Griffiths BJ, Zaehle T, Repplinger S, Schmitt FC, Voges J, Hanslmayr S, Staudigl T.
703 2022. Rhythmic interactions between the mediodorsal thalamus and prefrontal
704 cortex precede human visual perception. *Nature Communications 2022 13:1* **13**:1–
705 11. doi:10.1038/s41467-022-31407-z
706 Halassa MM, Sherman SM. 2019. Thalamo-cortical circuit motifs: a general framework.
707 *Neuron* **103**:762. doi:10.1016/J.NEURON.2019.06.005
708 Halverson HE, Freeman JH. 2010. Ventral lateral geniculate input to the medial pons is
709 necessary for visual eyeblink conditioning in rats. *Learn Mem* **17**:80–85.
710 doi:10.1101/LM.1572710
711 Herry C, Ferraguti F, Singewald N, Letzkus JJ, Ehrlich I, Lüthi A. 2010. Neuronal circuits
712 of fear extinction. *European Journal of Neuroscience* **31**:599–612.
713 doi:10.1111/J.1460-9568.2010.07101.X
714 Homman-Ludiye J, Bourne JA. 2019. The medial pulvinar: function, origin and
715 association with neurodevelopmental disorders. *J Anat* **235**:507–520.
716 doi:10.1111/JOA.12932
717 Hummos A, Wang BA, Drammis S, Halassa MM, Pleger B. 2022. Thalamic regulation of
718 frontal interactions in human cognitive flexibility. *PLoS Comput Biol* **18**:e1010500.
719 doi:10.1371/JOURNAL.PCBI.1010500
720 Hwang K, Bertolero MA, Liu WB, D'Esposito M. 2017. The Human Thalamus Is an
721 Integrative Hub for Functional Brain Networks. *Journal of Neuroscience* **37**:5594–
722 5607. doi:10.1523/JNEUROSCI.0067-17.2017
723 Hwang K, Bruss J, Tranel D, Boes AD. 2020. Network Localization of Executive
724 Function Deficits in Patients with Focal Thalamic Lesions. *J Cogn Neurosci*
725 **32**:2303. doi:10.1162/JOCN_A_01628
726 JASP Team. 2024. JASP (Versions 0.18.3 and 0.19.3).
727 Koller K, Rafal RD, Platt A, Mitchell ND. 2019. Orienting toward threat: Contributions of
728 a subcortical pathway transmitting retinal afferents to the amygdala via the superior

colliculus and pulvinar. *Neuropsychologia* **128**:78–86. doi:10.1016/J.NEUROPSYCHOLOGIA.2018.01.027

Kolling N, Wittmann M, Rushworth MFS. 2014. Multiple neural mechanisms of decision making and their competition under changing risk pressure. *Neuron* **81**:1190–1202. doi:10.1016/J.NEURON.2014.01.033/ATTACHMENT/A9984A25-8961-453B-8E1A-778EAD3A0ADE/MMC1.PDF

Konrad C, Neuhoff L, Adolph D, Goerigk S, Herbert JS, Jagusch-Poirier J, Weigelt S, Seehagen S, Schneider S. 2024. Associative learning via eyeblink conditioning differs by age from infancy to adulthood. *Communications Psychology 2024 2:1* **2**:1–13. doi:10.1038/s44271-024-00176-4

Korn CW, Bach DR. 2019. Minimizing threat via heuristic and optimal policies recruits hippocampus and medial prefrontal cortex. *Nature Human Behaviour 2019 3:7* **3**:733–745. doi:10.1038/s41562-019-0603-9

Korn CW, Bach DR. 2018. Heuristic and optimal policy computations in the human brain during sequential decision-making. *Nature Communications 2018 9:1* **9**:1–15. doi:10.1038/s41467-017-02750-3

Kragel PA, Čeko M, Theriault J, Chen D, Satpute AB, Wald LW, Lindquist MA, Feldman Barrett L, Wager TD. 2021. A human colliculus-pulvinar-amygdala pathway encodes negative emotion. *Neuron* **109**:2404-2412.e5. doi:10.1016/J.NEURON.2021.06.001/ATTACHMENT/2E7063C2-7363-4DE3-9A2B-F75C55D9DD96/MMC3.PDF

Krasne FB, Zinn R, Vissel B, Fanselow MS, Franklin Krasne CB, Howland-Rose V, Battersby D, King D. 2021. Extinction and discrimination in a Bayesian model of context fear conditioning (BaconX). *Hippocampus* **31**:790–814. doi:10.1002/HIPO.23298

Le Q Van, Isbell LA, Matsumoto J, Nguyen M, Hori E, Maior RS, Tomaz C, Tran AH, Ono T, Nishijo H. 2013. Pulvinar neurons reveal neurobiological evidence of past selection for rapid detection of snakes. *Proc Natl Acad Sci U S A* **110**:19000–19005. doi:10.1073/PNAS.1312648110/SUPPL_FILE/PNAS.201312648SI.PDF

LeDoux JE, Pine DS. 2016. Using Neuroscience to Help Understand Fear and Anxiety: A Two-System Framework. *https://doi.org/101176/appi.ajp201616030353* **173**:1083–1093. doi:10.1176/APPI.AJP.2016.16030353

Lee S, Shin HS. 2016. The role of mediodorsal thalamic nucleus in fear extinction. *J Anal Sci Technol* **7**:1–5. doi:10.1186/S40543-016-0093-6/FIGURES/1

Lee Sukchan, Ahmed T, Lee Soojung, Kim H, Choi S, Kim DS, Kim SJ, Cho J, Shin HS. 2011. Bidirectional modulation of fear extinction by mediodorsal thalamic firing in mice. *Nature Neuroscience 2011 15:2* **15**:308–314. doi:10.1038/nn.2999

Li K, Fan L, Cui Y, Wei X, He Y, Yang J, Lu Y, Li W, Shi W, Cao L, Cheng L, Li A, You B, Jiang T. 2022. The human mediodorsal thalamus: Organization, connectivity, and function. *Neuroimage* **249**:118876. doi:10.1016/J.NEUROIMAGE.2022.118876

Li XB, Inoue T, Nakagawa S, Koyama T. 2004. Effect of mediodorsal thalamic nucleus lesion on contextual fear conditioning in rats. *Brain Res* **1008**:261–272. doi:10.1016/J.BRAINRES.2004.02.038

Lithari C, Moratti S, Weisz N. 2015. Thalamocortical interactions underlying visual fear conditioning in humans. *Hum Brain Mapp* **36**:4592. doi:10.1002/HBM.22940

Mahoney HL, Schmidt TM. 2024. The cognitive impact of light: illuminating ipRGC circuit mechanisms. *Nature Reviews Neuroscience 2024 25:3* **25**:159–175. doi:10.1038/s41583-023-00788-5

Maren S. 2001. Nuerobiology of Pavlovian fear conditioning. *Annu Rev Neurosci* **24**:897–931. doi:10.1146/ANNUREV.NEURO.24.1.897/CITE/REFWORKS

Maren S, Phan KL, Liberzon I. 2013. The contextual brain: implications for fear conditioning, extinction and psychopathology. *Nature Reviews Neuroscience 2013 14:6* **14**:417–428. doi:10.1038/nrn3492

Maren S, Quirk GJ. 2004. Neuronal signalling of fear memory. *Nature Reviews Neuroscience 2004 5:11* **5**:844–852. doi:10.1038/nrn1535

Marin MF, Hammoud MZ, Klumpp H, Simon NM, Milad MR. 2020. Multimodal Categorical and Dimensional Approaches to Understanding Threat Conditioning and Its Extinction in Individuals With Anxiety Disorders. *JAMA Psychiatry* **77**:618–627. doi:10.1001/JAMAPSYCHIATRY.2019.4833

McFadyen J, Mattingley JB, Garrido MI. 2019. An afferent white matter pathway from the pulvinar to the amygdala facilitates fear recognition. *Elife* **8**. doi:10.7554/ELIFE.40766

Milad MR, Furtak SC, Greenberg JL, Keshaviah A, Im JJ, Falkenstein MJ, Jenike M, Rauch SL, Wilhelm S. 2013. Deficits in Conditioned Fear Extinction in Obsessive-Compulsive Disorder and Neurobiological Changes in the Fear Circuit. *JAMA Psychiatry* **70**:608–618. doi:10.1001/JAMAPSYCHIATRY.2013.914

Milad MR, Pitman RK, Ellis CB, Gold AL, Shin LM, Lasko NB, Zeidan MA, Handwerger K, Orr SP, Rauch SL. 2009. Neurobiological Basis of Failure to Recall Extinction Memory in Posttraumatic Stress Disorder. *Biol Psychiatry* **66**:1075–1082. doi:10.1016/J.BIOPSYCH.2009.06.026

Milad MR, Quirk GJ. 2012. Fear Extinction as a Model for Translational Neuroscience: Ten Years of Progress. *Annu Rev Psychol* **63**:129. doi:10.1146/ANNUREV.PSYCH.121208.131631

Milad MR, Quirk GJ. 2002. Neurons in medial prefrontal cortex signal memory for fear extinction. *Nature 2002 420:6911* **420**:70–74. doi:10.1038/nature01138

Milad MR, Rosenbaum BL, Simon NM. 2014. Neuroscience of fear extinction: Implications for assessment and treatment of fear-based and anxiety related disorders. *Behaviour Research and Therapy* **62**:17–23. doi:10.1016/J.BRAT.2014.08.006

Milad MR, Wright CI, Orr SP, Pitman RK, Quirk GJ, Rauch SL. 2007. Recall of fear extinction in humans activates the ventromedial prefrontal cortex and hippocampus in concert. *Biol Psychiatry* **62**:446–454. doi:10.1016/J.BIOPSYCH.2006.10.011

Mukherjee A, Lam NH, Wimmer RD, Halassa MM. 2021. Thalamic circuits for independent control of prefrontal signal and noise. *Nature 2021 600:7887* **600**:100–104. doi:10.1038/s41586-021-04056-3

Nejati V, Majdi R, Salehinejad MA, Nitsche MA. 2021. The role of dorsolateral and ventromedial prefrontal cortex in the processing of emotional dimensions. *Scientific Reports 2021 11:1* **11**:1–12. doi:10.1038/s41598-021-81454-7

Nieto-Castanon A. 2020. FMRI denoising pipeline. *Handbook of functional connectivity Magnetic Resonance Imaging methods in CONN* 17–25. doi:10.56441/HILBERTPRESS.2207.6600

Nieto-Castanon A, Whitfield-Gabrieli S. 2022. CONN functional connectivity toolbox: RRID SCR_009550, release 22. *CONN functional connectivity toolbox: RRID SCR_009550, release 22*. doi:10.56441/HILBERTPRESS.2246.5840

O'Connor DH, Fukui MM, Pinsk MA, Kastner S. 2002. Attention modulates responses in the human lateral geniculate nucleus. *Nature Neuroscience 2002 5:11* **5**:1203–1209. doi:10.1038/nn957

Pavlov I. 1904. Nobel Lecture. NobelPrize.org. Available at: https://www.nobelprize.org/prizes/medicine/1904/pavlov/lecture/

Paydar A, Lee B, Gangadharan G, Lee S, Hwang EM, Shin HS. 2014. Extrasynaptic GABAA receptors in mediodorsal thalamic nucleus modulate fear extinction learning. *Mol Brain* **7**:39. doi:10.1186/1756-6606-7-39

Penzo MA, Robert V, Tucciarone J, De Bundel D, Wang M, Van Aelst L, Darvas M, Parada LF, Palmiter RD, He M, Huang ZJ, Li B. 2015. The paraventricular thalamus controls a central amygdala fear circuit. *Nature* **519**:455–459. doi:10.1038/NATURE13978

Pessoa L, Adolphs R. 2010. Emotion processing and the amygdala: from a "low road" to "many roads" of evaluating biological significance. *Nature Reviews Neuroscience 2010 11:11* **11**:773–782. doi:10.1038/nrn2920

Phelps EA, LeDoux JE. 2005. Contributions of the amygdala to emotion processing: From animal models to human behavior. *Neuron* **48**:175–187. doi:10.1016/J.NEURON.2005.09.025/ASSET/31E14E48-ACAC-4132-ACD2-31705A61F19C/MAIN.ASSETS/GR4.JPG

Rafal RD, Koller K, Bultitude JH, Mullins P, Ward R, Mitchell AS, Bell AH. 2015. Connectivity between the superior colliculus and the amygdala in humans and macaque monkeys: virtual dissection with probabilistic DTI tractography. *J Neurophysiol* **114**:1947–1962. doi:10.1152/JN.01016.2014

Ramanathan KR, Jin J, Giustino TF, Payne MR, Maren S. 2018. Prefrontal projections to the thalamic nucleus reuniens mediate fear extinction. *Nature Communications 2018 9:1* **9**:1–12. doi:10.1038/s41467-018-06970-z

Ramanathan KR, Maren S. 2019. Nucleus reuniens mediates the extinction of contextual fear conditioning. *Behavioural Brain Research* **374**:112114. doi:10.1016/J.BBR.2019.112114

Ratigan HC, Krishnan S, Smith S, Sheffield MEJ. 2023. A thalamic-hippocampal CA1 signal for contextual fear memory suppression, extinction, and discrimination. *Nature Communications 2023 14:1* **14**:1–17. doi:10.1038/s41467-023-42429-6

Rolls ET, Huang CC, Lin CP, Feng J, Joliot M. 2020. Automated anatomical labelling atlas 3. *Neuroimage* **206**. doi:10.1016/J.NEUROIMAGE.2019.116189

Saalmann YB, Kastner S. 2011. Cognitive and Perceptual Functions of the Visual Thalamus. *Neuron* **71**:209. doi:10.1016/J.NEURON.2011.06.027

Saalmann YB, Kastner S. 2009. Gain control in the visual thalamus during perception and cognition. *Curr Opin Neurobiol* **19**:408. doi:10.1016/J.CONB.2009.05.007

Salay LD, Huberman AD. 2021. Divergent outputs of the ventral lateral geniculate nucleus mediate visually evoked defensive behaviors. *Cell Rep* **37**. doi:10.1016/j.celrep.2021.109792

Sherman SM. 2016. Thalamus plays a central role in ongoing cortical functioning. *Nature Neuroscience 2016 19:4* **19**:533–541. doi:10.1038/nn.4269

Sherman SM. 2007. The thalamus is more than just a relay. *Curr Opin Neurobiol* **17**:417–422. doi:10.1016/J.CONB.2007.07.003

Sherman SMurray, Guillery RW. 2006. Exploring the thalamus and its role in cortical function 484.

Shi C, Davis M. 2001. Visual pathways involved in fear conditioning measured with fear-potentiated startle: behavioral and anatomic studies. *J Neurosci* **21**:9844–9855. doi:10.1523/JNEUROSCI.21-24-09844.2001

Silverstein DN, Ingvar M. 2015. A multi-pathway hypothesis for human visual fear signaling. *Front Syst Neurosci* **9**:137726. doi:10.3389/FNSYS.2015.00101/PDF

Steinmetz AB, Buss EW, Freeman JH. 2013. Inactivation of the ventral lateral geniculate and nucleus of the optic tract impairs retention of visual eyeblink conditioning. *Behavioral Neuroscience* **127**:690–693. doi:10.1037/A0033729

Takakuwa N, Isa K, Onoe H, Takahashi J, Isa T. 2021. Contribution of the Pulvinar and Lateral Geniculate Nucleus to the Control of Visually Guided Saccades in Blindsight Monkeys. *Journal of Neuroscience* **41**:1755–1768. doi:10.1523/JNEUROSCI.2293-20.2020

Totty MS, Tuna T, Ramanathan KR, Jin J, Peters SE, Maren S. 2023. Thalamic nucleus reuniens coordinates prefrontal-hippocampal synchrony to suppress extinguished fear. *Nature Communications 2023 14:1* **14**:1–12. doi:10.1038/s41467-023-42315-1

Tovote P, Fadok JP, Lüthi A. 2015. Neuronal circuits for fear and anxiety. *Nature Reviews Neuroscience 2015 16:6* **16**:317–331. doi:10.1038/nrn3945

Vuilleumier P, Armony JL, Driver J, Dolan RJ. 2003. Distinct spatial frequency sensitivities for processing faces and emotional expressions. *Nature Neuroscience 2003 6:6* **6**:624–631. doi:10.1038/nn1057

Ward R, Danziger S, Bamford S. 2005. Response to visual threat following damage to the pulvinar. *Curr Biol* **15**:571–573. doi:10.1016/J.CUB.2005.01.056

Wei P, Liu N, Zhang Z, Liu X, Tang Y, He X, Wu B, Zhou Z, Liu Y, Li J, Zhang Y, Zhou X, Xu L, Chen L, Bi G, Hu X, Xu F, Wang L. 2015. Processing of visually evoked innate fear by a non-canonical thalamic pathway. *Nature Communications 2015 6:1* **6**:1–13. doi:10.1038/ncomms7756

Wen Z, Pace-Schott EF, Lazar SW, Rosén J, Åhs F, Phelps EA, LeDoux JE, Milad MR. 2024. Distributed neural representations of conditioned threat in the human brain. *Nature Communications 2024 15:1* **15**:1–14. doi:10.1038/s41467-024-46508-0

Wen Z, Raio CM, Pace-Schott EF, Lazar SW, LeDoux JE, Phelps EA, Milad MR. 2022. Temporally and anatomically specific contributions of the human amygdala to threat and safety learning. *Proc Natl Acad Sci U S A* **119**:e2204066119. doi:10.1073/PNAS.2204066119/SUPPL_FILE/PNAS.2204066119.SAPP.PDF

Whitfield-Gabrieli S, Nieto-Castanon A. 2012. Conn: a functional connectivity toolbox for correlated and anticorrelated brain networks. *Brain Connect* **2**:125–141. doi:10.1089/BRAIN.2012.0073

Whyte CJ, Redinbaugh MJ, Shine JM, Saalmann YB. 2024. Thalamic contributions to the state and contents of consciousness. *Neuron* **112**:1611–1625. doi:10.1016/J.NEURON.2024.04.019/ASSET/AA96B159-0E29-4D7D-B3C8-E302EA442A73/MAIN.ASSETS/GR2.JPG

Wolff M, Halassa MM. 2024. The mediodorsal thalamus in executive control. *Neuron* **112**:893–908. doi:10.1016/J.NEURON.2024.01.002/ASSET/8EBBDE5D-737B-479F-966E-07AE8F092DB6/MAIN.ASSETS/GR3.JPG

Wurtz RH, McAlonan K, Cavanaugh J, Berman RA. 2011. Thalamic pathways for active vision. *Trends Cogn Sci* **15**:177–184. doi:10.1016/J.TICS.2011.02.004

Yarkoni T, Poldrack RA, Nichols TE, Van Essen DC, Wager TD. 2011. Large-scale automated synthesis of human functional neuroimaging data. *Nature Methods 2011 8:8* **8**:665–670. doi:10.1038/nmeth.1635

Zheng C, Huang Y, Bo B, Wei L, Liang Z, Wang Z. 2020. Projection from the Anterior Cingulate Cortex to the Lateral Part of Mediodorsal Thalamus Modulates Vicarious Freezing Behavior. *Neurosci Bull* **36**:217–229. doi:10.1007/S12264-019-00427-Z/METRICS

933 **Figure captions**

934 **Fig 1. Neural representation of associative threat learning in pulvinar divisions, MD**
935 **and LGN.**

936 **a.** Human fear conditioning paradigm in the fMRI. **b-d.** Means ± SE of activation in
937 response to CS+ vs. CS- at both block-wise and trial-wise levels within the pulvinar
938 divisions (**b**), MD (**c**), and LGN (**d**). **e.** ROI-to-ROI connectivity. Right: the red line
939 represents significant positive connectivity to CS+ vs. CS- ($P_{FDR} < 0.05$), while the gray
940 lines indicate non-significant connectivity. Thalamic nuclei that showed no significant
941 connectivity with other regions (i.e., amygdala, hippocampus, etc.) were omitted from the
942 visualization. Left: boxplots and kernel density estimates illustrate the distribution of
943 connectivity values in response to CS+ and CS-.

944 SE: Standard error.

945 MD: Mediodorsal thalamus.

946 LGN: Lateral geniculate nucleus.

947 CS+ vs. CS-: Conditioned stimulus predicting shock vs. no shock.

948 ROI: Region of interest.

949 *p<0.05, **p<0.01, ***p<0.001

950 Display items in panel **a** were created using BioRender (BioRender.com).

951 **Fig 2. Quantifying the relationships between the anterior pulvinar and MD during**
952 **conditioning.**

953 **a.** Hierarchical regression models of trial-wise relationships between the anterior pulvinar
954 and MD activations while controlling for a potential effect of anatomical proximity. The
955 effect of anatomical proximity was controlled by progressively adding other pulvinar
956 divisions as controls. **b.** Results of a hierarchical model that included the LGN as an
957 alternative control, distinct from the pulvinar. **c.** Comparison of activation levels in the
958 anterior pulvinar and MD at both block-wise and trial-wise levels (means ± SE).

959 *p<0.05, **p<0.01, ***p<0.001

960 MD: Mediodorsal thalamus.

961 LGN: Lateral geniculate nucleus.

962 SE: Standard error.

963

964

965

966

967

968

969 **Fig 3. A data-driven approach to understanding the functional relationships**
970 **between pulvinar divisions during conditioning**

971 **a.** Means ± SE of activation differences between pulvinar divisions. **b.** Network analysis
972 reveals that the medial pulvinar serves as a central hub, mediating interactions among
973 pulvinar divisions and exhibiting increased centrality measures. **c.** Schematic
974 visualization of activation patterns we observed in pulvinar divisions. **d.** Previous studies
975 suggest that the inferior and lateral pulvinar are involved in processing basic visual
976 information, while the medial pulvinar is associated with higher-level functions, including
977 working memory. **e.** Based on **b-d**, we hypothesize that the medial pulvinar mediates the
978 relationships with other divisions. **f.** Mediation analysis supports our hypothesis (panel **e**).
979 **g.** Validation of the mediation model on an additional independent sample. Dashed paths
980 in panels **f** and **g** represent statistically unstable paths, while the continuous paths
981 indicate stable paths.

982 SE: Standard error.

983 SC: Superior colliculus.

984 *p<0.05, **p<0.01, ***p<0.001

985 Display items in panels **d** and **e** were created using BioRender (BioRender.com).

986

987

988

989 **Fig 4. Neural representation of extinction learning in pulvinar divisions, MD and**
990 **LGN.**

991 **a.** Human extinction learning paradigm in the fMRI. **b-d.** Means ± SE of activation in
992 response to extinguished CS+ vs. CS- at both block-wise and trial-wise levels within the
993 pulvinar divisions (**b**), MD (**c**), and LGN (**d**). **e.** ROI-to-ROI connectivity. Right: the red line
994 represents significant positive connectivity to extinguished CS+ vs. CS- ($P_{FDR} < 0.05$),
995 while the gray lines indicate no significant connectivity. Thalamic nuclei that showed non-
996 significant connectivity with other regions (i.e., amygdala, hippocampus, etc.) were
997 omitted from the visualization. Left: boxplots and kernel density estimates illustrate the
998 distribution of connectivity values in response to extinguished CS+ and CS-.

999 SE: Standard error.

1000 MD: Mediodorsal thalamus.

1001 LGN: Lateral geniculate nucleus.

1002 Extinguished CS+ vs. CS-: A conditioned stimulus that no longer predicts shock vs. a
1003 stimulus that was never paired with shock.

1004 ROI: Region of interest.

1005 *p<0.05, **p<0.01, ***p<0.001

1006 Display items in panel **a** were created using BioRender (BioRender.com).

1007

1008 **Fig 5. Neural representation of extinction recall in pulvinar divisions, MD and LGN.**

1009 **a.** Human extinction recall paradigm in the fMRI conducted within safe contextual cues.
1010 **b-d.** Means ± SE of activation in response to extinguished CS+ vs. CS- at both block-
1011 wise and trial-wise levels within the pulvinar divisions (**b**), MD (**c**), and LGN (**d**). **e.** ROI-
1012 to-ROI connectivity. Right: the red line represents significant positive connectivity to
1013 extinguished CS+ vs. CS- ($P_{FDR} < 0.05$), while the gray lines indicate non-significant
1014 connectivity. Thalamic nuclei that showed no significant connectivity with other regions
1015 (i.e., amygdala, hippocampus, etc.) were omitted from the visualization. Left: boxplots and
1016 kernel density estimates illustrate the distribution of connectivity values in response to
1017 extinguished CS+ and CS-.

1018 SE: Standard error.

1019 MD: Mediodorsal thalamus.

1020 LGN: Lateral geniculate nucleus.

1021 Extinguished CS+ vs. CS-: A conditioned stimulus that no longer predicts shock vs. a
1022 stimulus that was never paired with shock.

1023 ROI: Region of interest.

1024 *p<0.05, **p<0.01, ***p<0.001

1025 Display items in panel **a** were created using BioRender (BioRender.com).

1026

1027 **Fig 6. Neural representation of threat renewal in pulvinar divisions, MD and LGN.**

1028 **a.** Human threat renewal paradigm in the fMRI conducted within threat contextual cues in
1029 the original context where fear conditioning occurred. **b-d.** Means ± SE of activation in
1030 response to extinguished CS+ vs. CS- at both block-wise and trial-wise levels within the
1031 pulvinar divisions (**b**), MD (**c**), and LGN (**d**). **e.** ROI-to-ROI connectivity. Right: the red line
1032 represents significant positive connectivity to extinguished CS+ vs. CS- ($P_{FDR} < 0.05$),
1033 while the gray lines indicate non-significant connectivity. Thalamic nuclei that showed no
1034 significant connectivity with other regions (i.e., amygdala, hippocampus, etc.) were
1035 omitted from the visualization. Left: boxplots and kernel density estimates illustrate the
1036 distribution of connectivity values in response to extinguished CS+ and CS-.

1037 SE: Standard error.

1038 MD: Mediodorsal thalamus.

1039 LGN: Lateral geniculate nucleus.

1040 Extinguished CS+ vs. CS-: A conditioned stimulus that no longer predicts shock vs. a
1041 stimulus that was never paired with shock.

1042 ROI: Region of interest.

1043 *p<0.05, **p<0.01, ***p<0.001

1044 Display items in panel **a** were created using BioRender (BioRender.com).

1045

1046 **Fig 7. Neurobehavioral models of thalamic involvement in associative threat**
1047 **learning and memory.**

1048 **a.** Schematic illustration of thalamic circuitry during the acquisition of associative threat
1049 learning, highlighting interactions between pulvinar divisions, MD, and LGN with key brain
1050 regions involved in fear expression.

1051 **b.** A thalamic-dependent "toggle switch" regulates the retrieval of safety vs. threat-related
1052 memory. The MD-dACC connectivity modulates the interaction between dACC and
1053 vmPFC, promoting vmPFC dominance during extinction recall. In contrast, the anterior
1054 pulvinar-vmPFC connectivity promotes dACC dominance, enhancing the expression of
1055 threat memory during threat renewal.

1056 MD: Mediodorsal thalamus.

1057 LGN: Lateral geniculate nucleus.

1058 vmPFC = Ventromedial prefrontal cortex.

1059 dACC = Dorsal anterior cingulate cortex.

1060 V1, V2, and V4: Primary, secondary, and fourth visual areas.
1061 TEO, TE: Temporal cortex regions.
1062 Hypo.: Hypothalamus.
1063 Hippo.: Hippocampus.

1064

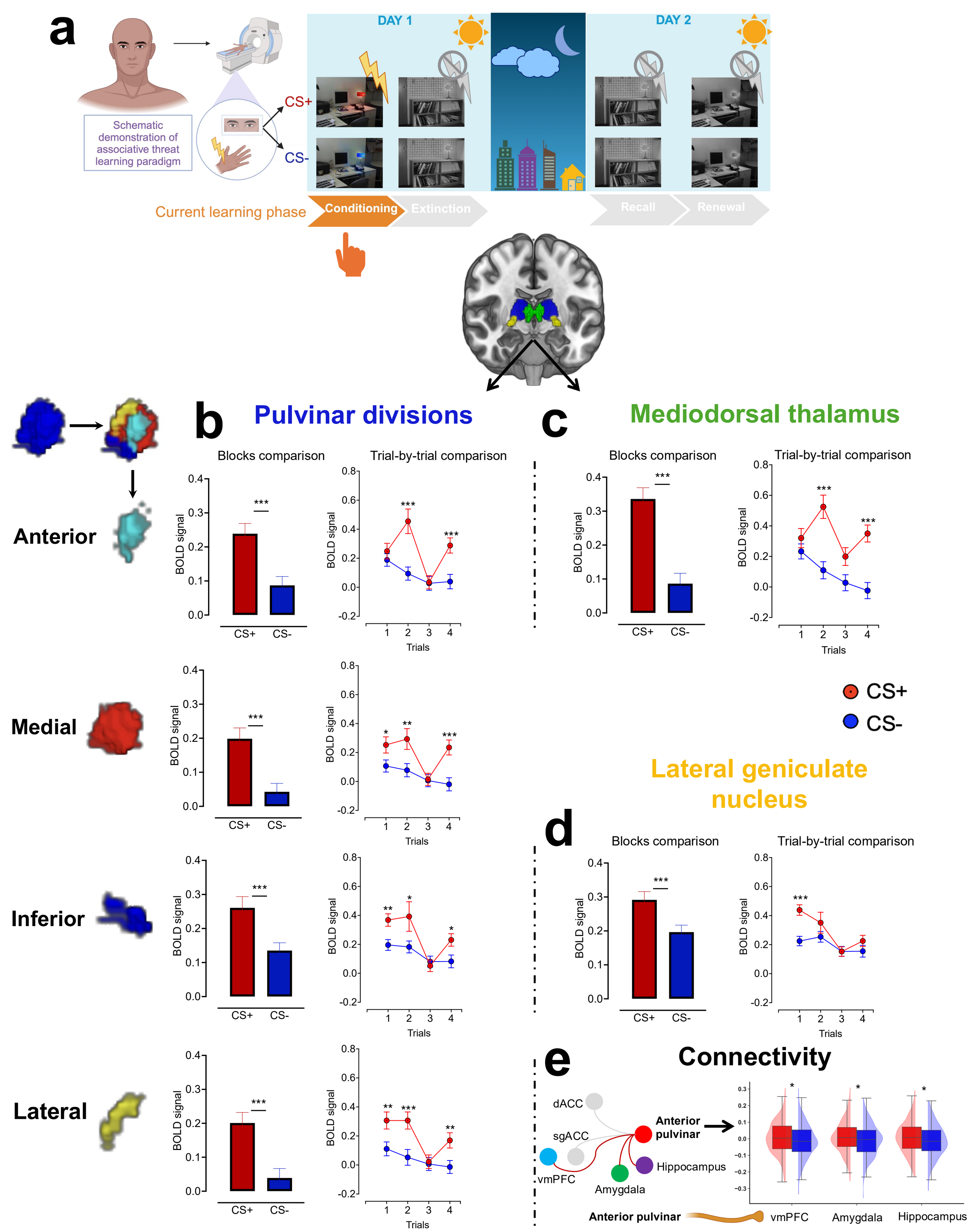
a
Schematic demonstration of associative threat learning paradigm
CS+
CS-
DAY 1
DAY 2
Current learning phase
Conditioning
Extinction
Recall
Renewal
b
Pulvinar divisions
Anterior
Medial
Inferior
Lateral
Blocks comparison
Trial-by-trial comparison
BOLD signal
Trials
CS+
CS-
c
Mediodorsal thalamus
Lateral geniculate nucleus
d
e
Connectivity
dACC
sgACC
vmPFC
Amygdala
Anterior pulvinar
Hippocampus

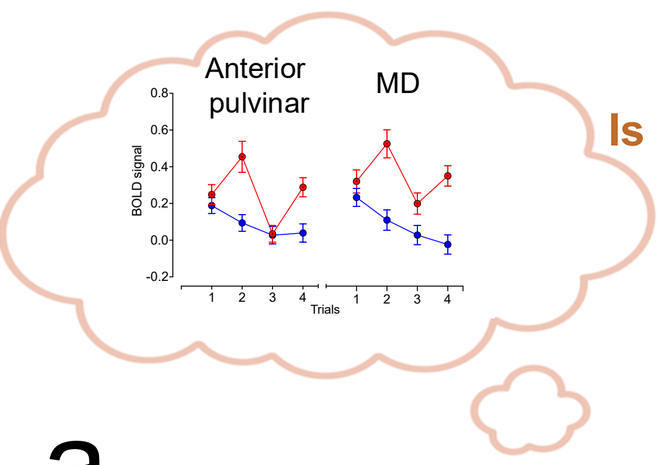

Is the observed similarity in activation between the anterior pulvinar and MD statistically significant, or could it be attributed to anatomical proximity?

Anterior pulvinar · Lateral pulvinar · Inferior pulvinar · Medial pulvinar · LGN

Hierarchical regression

a

Conservative control: Other pulvinar divisions

Alternative control: LGN

b

Raw correlation | Standard β estimations | 1x10⁴ bootstraps β estimations | R² change | 1x10⁴ bootstraps β estimations

Trial 1

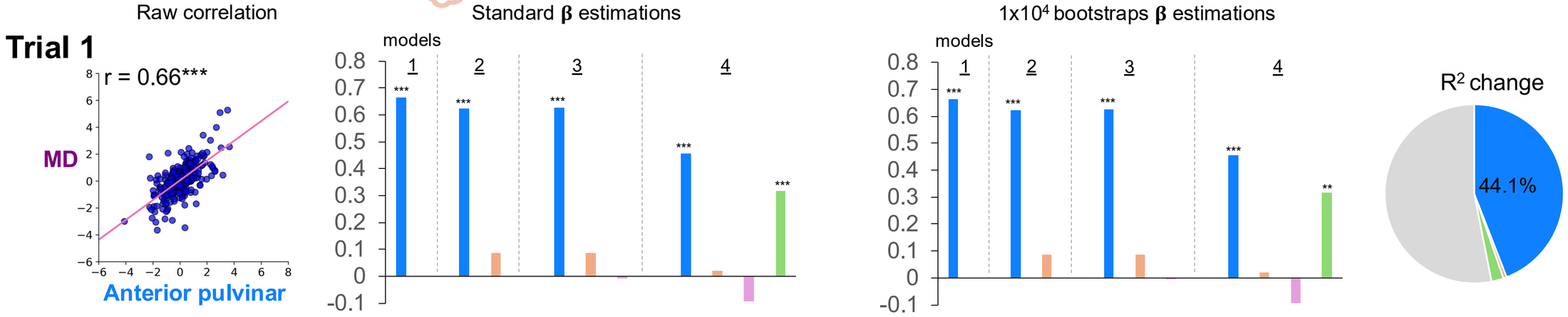

Trial 2

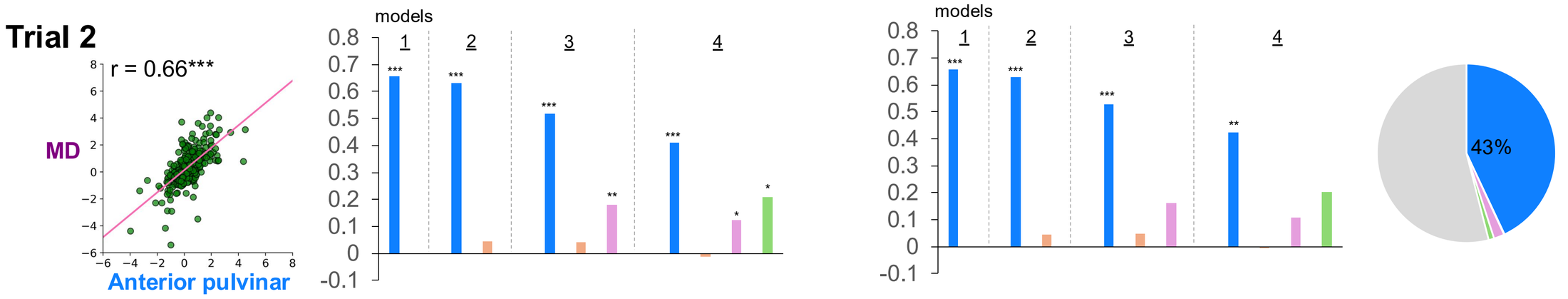

Trial 3

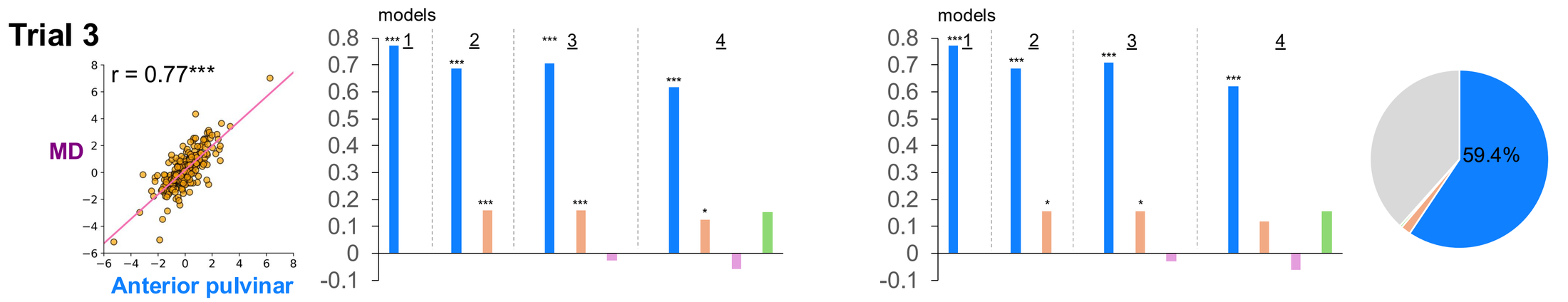

Trial 4

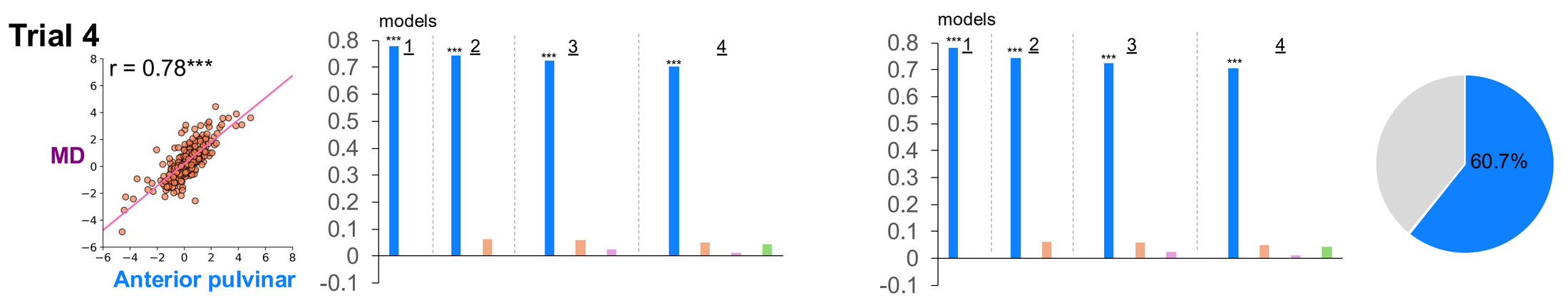

R^2 change = 0.006

R^2 change = 0.01

R^2 change = 0.03

R^2 change = 0.001

C **Are the activation levels significantly different between anterior pulvinar and MD?**

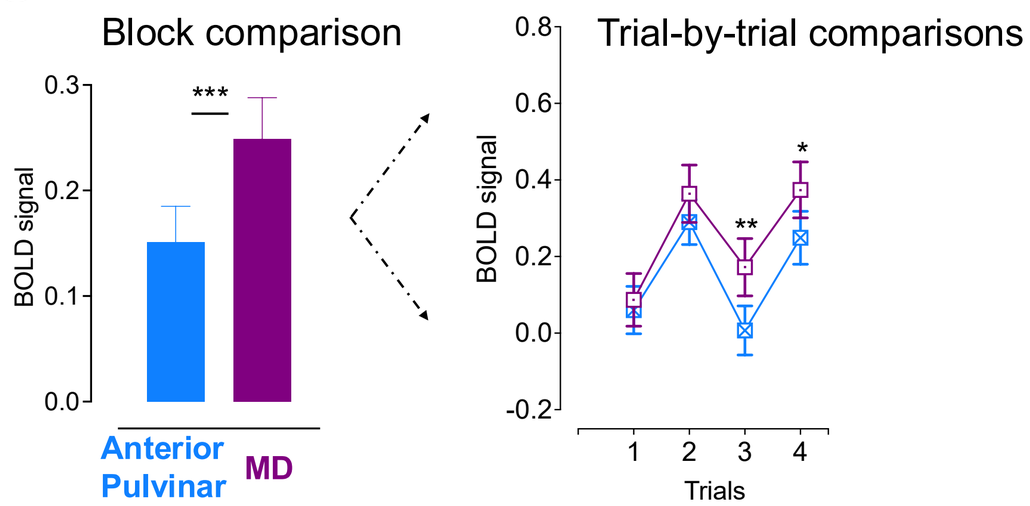

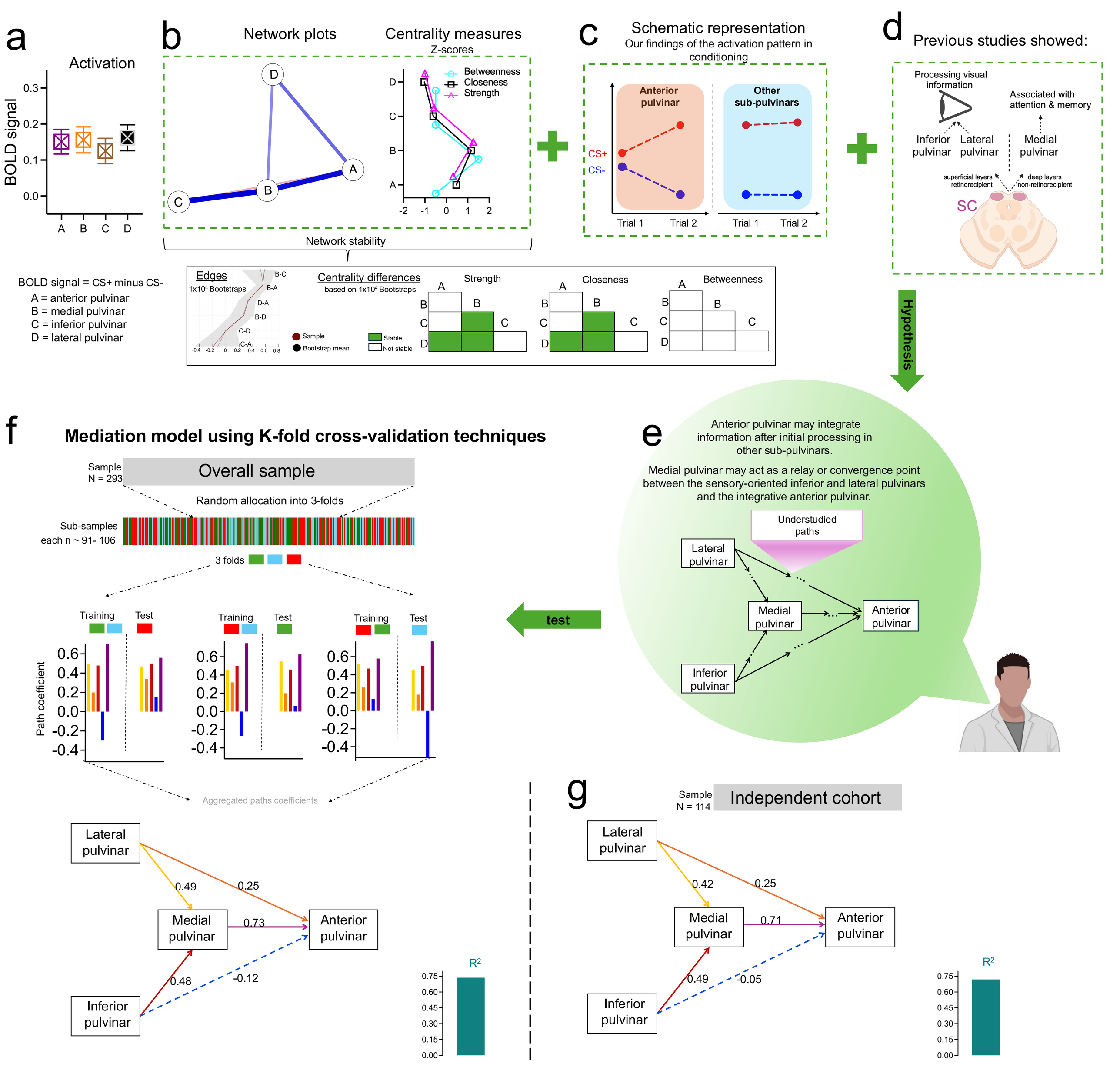
a
Activation
BOLD signal
0.3
0.2
0.1
0.0
A B C D
b
Network plots
Centrality measures
Z-scores
Betweenness
Closeness
Strength
Network stability
Edges
1x10⁴ Bootstraps
Centrality differences
based on 1x10⁴ Bootstraps
Sample
Bootstrap mean
Stable
Not stable
Strength
Closeness
Betweenness
BOLD signal = CS+ minus CS-
A = anterior pulvinar
B = medial pulvinar
C = inferior pulvinar
D = lateral pulvinar
c
Schematic representation
Our findings of the activation pattern in conditioning
Anterior pulvinar
Other sub-pulvinars
CS+
CS-
Trial 1
Trial 2
d
Previous studies showed:
Processing visual information
Associated with attention & memory
Inferior pulvinar
Lateral pulvinar
Medial pulvinar
superficial layers retinorecipient
deep layers non-retinorecipient
SC
Hypothesis
e
Anterior pulvinar may integrate information after initial processing in other sub-pulvinars.
Medial pulvinar may act as a relay or convergence point between the sensory-oriented inferior and lateral pulvinars and the integrative anterior pulvinar.
Understudied paths
Lateral pulvinar
Medial pulvinar
Anterior pulvinar
Inferior pulvinar
f
Mediation model using K-fold cross-validation techniques
Sample
N = 293
Overall sample
Random allocation into 3-folds
Sub-samples
each n ~ 91- 106
3 folds
Training
Test
Path coefficient
Aggregated paths coefficients
test
Lateral pulvinar
Medial pulvinar
Anterior pulvinar
Inferior pulvinar
0.49
0.25
0.73
0.48
-0.12
R²
g
Sample
N = 114
Independent cohort
Lateral pulvinar
Medial pulvinar
Anterior pulvinar
Inferior pulvinar
0.42
0.25
0.71
0.49
-0.05
R²

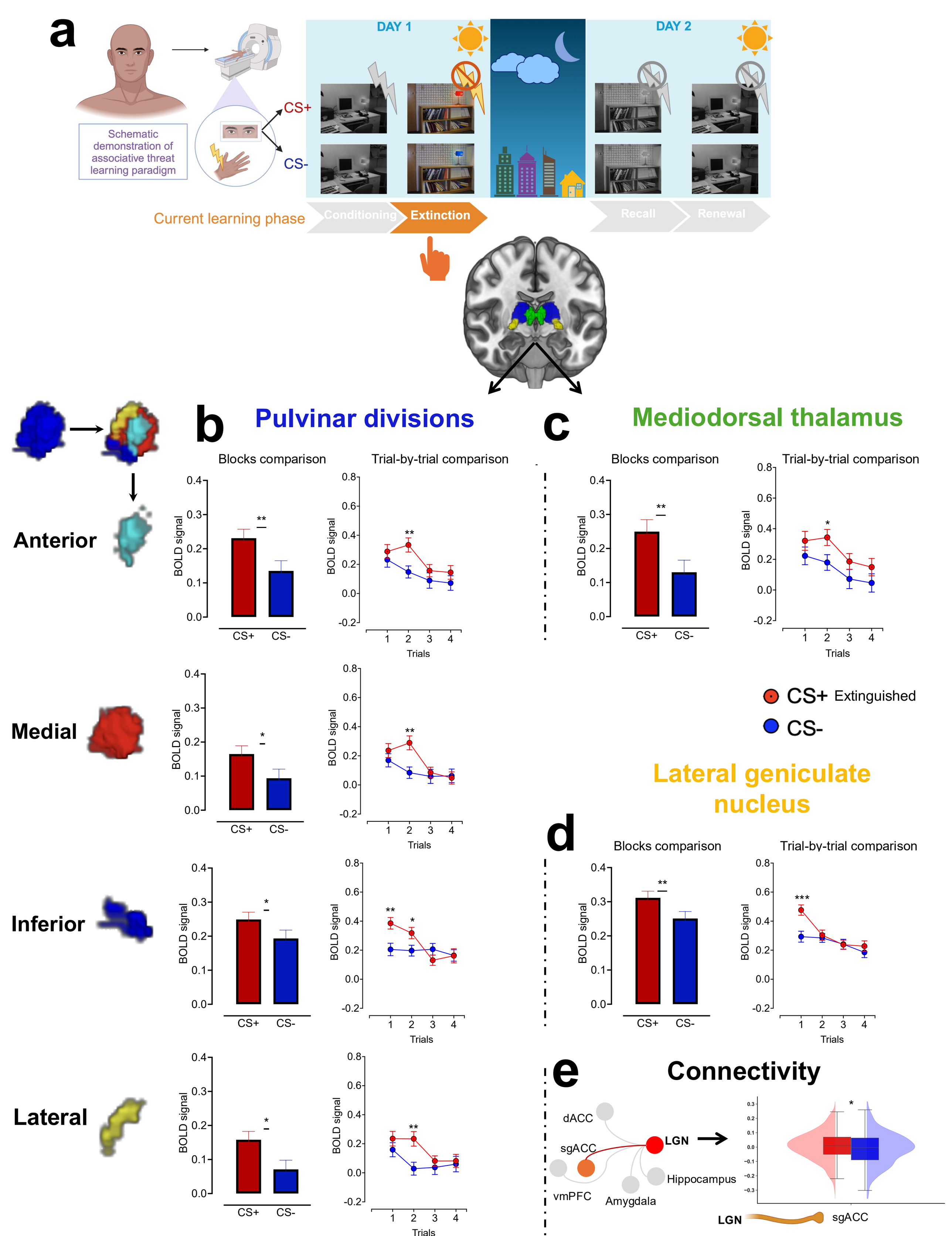
a
Schematic demonstration of associative threat learning paradigm
CS+
CS-
DAY 1
DAY 2
Current learning phase
Conditioning
Extinction
Recall
Renewal
b
Pulvinar divisions
Anterior
Medial
Inferior
Lateral
Blocks comparison
Trial-by-trial comparison
BOLD signal
Trials
c
Mediodorsal thalamus
CS+ Extinguished
CS-
Lateral geniculate nucleus
d
e
Connectivity
dACC
sgACC
LGN
Hippocampus
vmPFC
Amygdala
LGN
sgACC

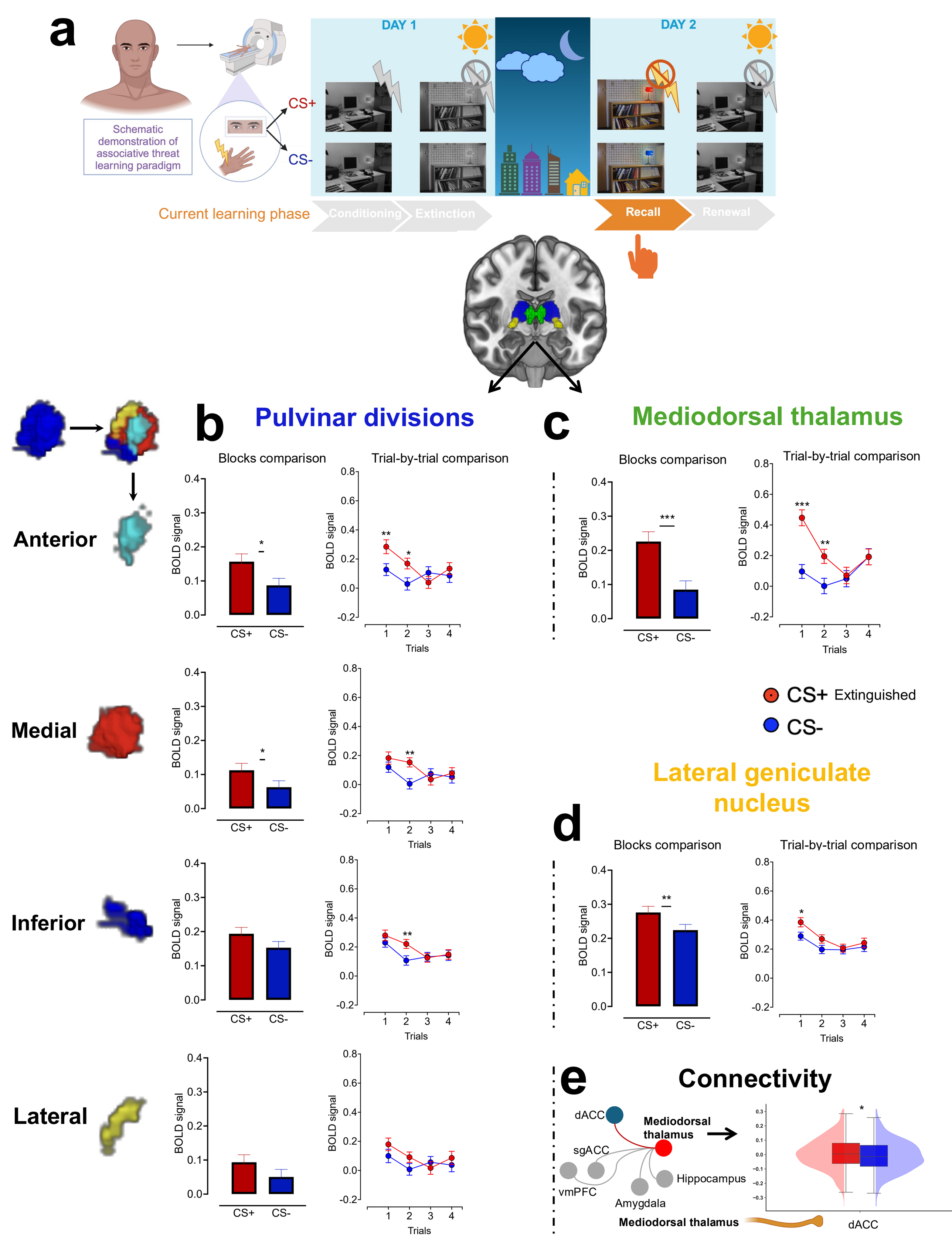
a
Schematic demonstration of associative threat learning paradigm
CS+
CS-
DAY 1
DAY 2
Current learning phase
Conditioning
Extinction
Recall
Renewal
b
Pulvinar divisions
Anterior
Medial
Inferior
Lateral
Blocks comparison
Trial-by-trial comparison
BOLD signal
CS+
CS-
Trials
c
Mediodorsal thalamus
CS+ Extinguished
CS-
Lateral geniculate nucleus
d
e
Connectivity
dACC
Mediodorsal thalamus
sgACC
vmPFC
Amygdala
Hippocampus
Mediodorsal thalamus
dACC

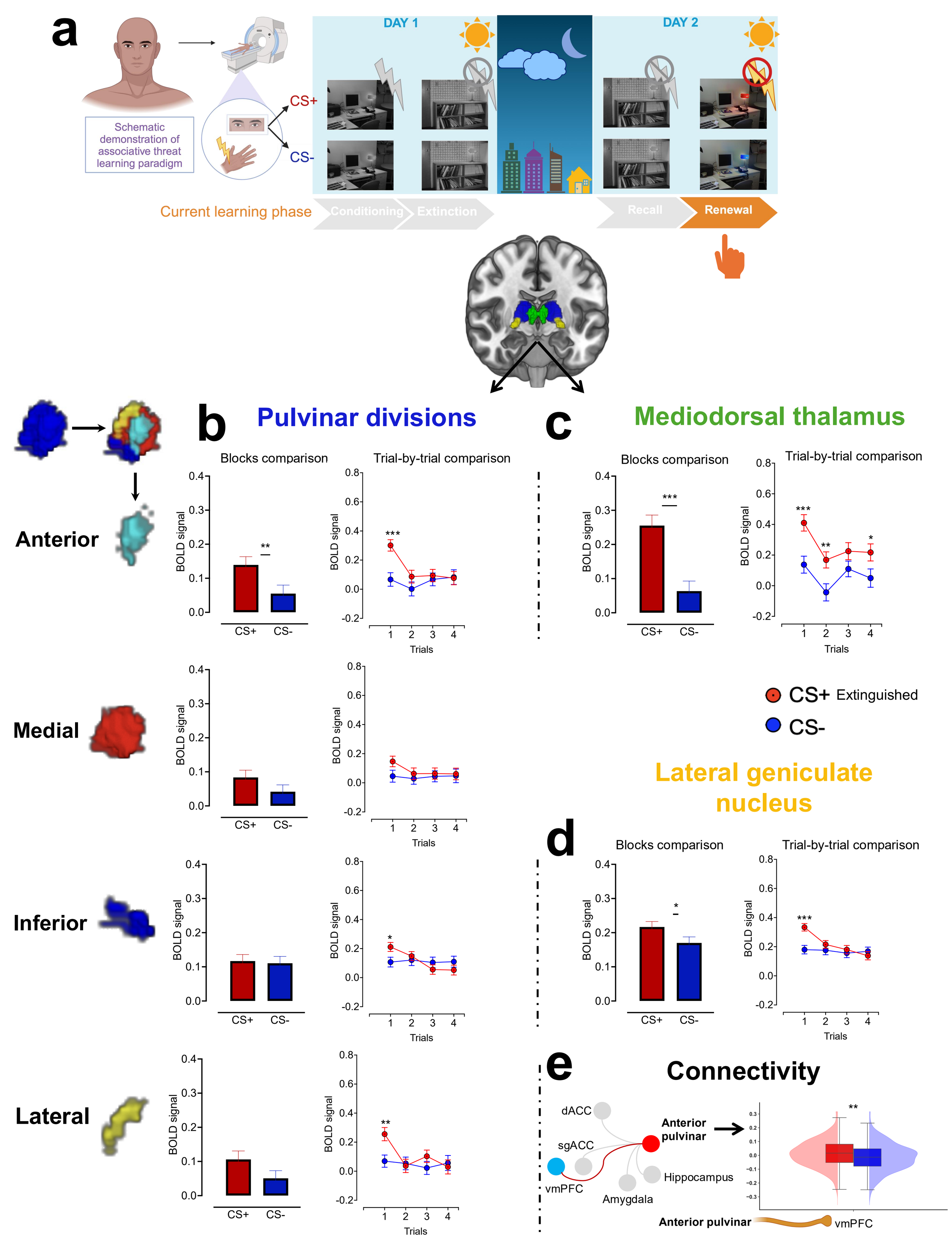
a
Schematic demonstration of associative threat learning paradigm
CS+
CS-
DAY 1
DAY 2
Current learning phase
Conditioning
Extinction
Recall
Renewal
b
Pulvinar divisions
Anterior
Medial
Inferior
Lateral
Blocks comparison
Trial-by-trial comparison
BOLD signal
Trials
CS+
CS-
c
Mediodorsal thalamus
CS+ Extinguished
CS-
Lateral geniculate nucleus
d
e
Connectivity
dACC
sgACC
vmPFC
Amygdala
Hippocampus
Anterior pulvinar
vmPFC

a Integrative simplified functional thalamic circuitry during the acquisition of associative threat learning

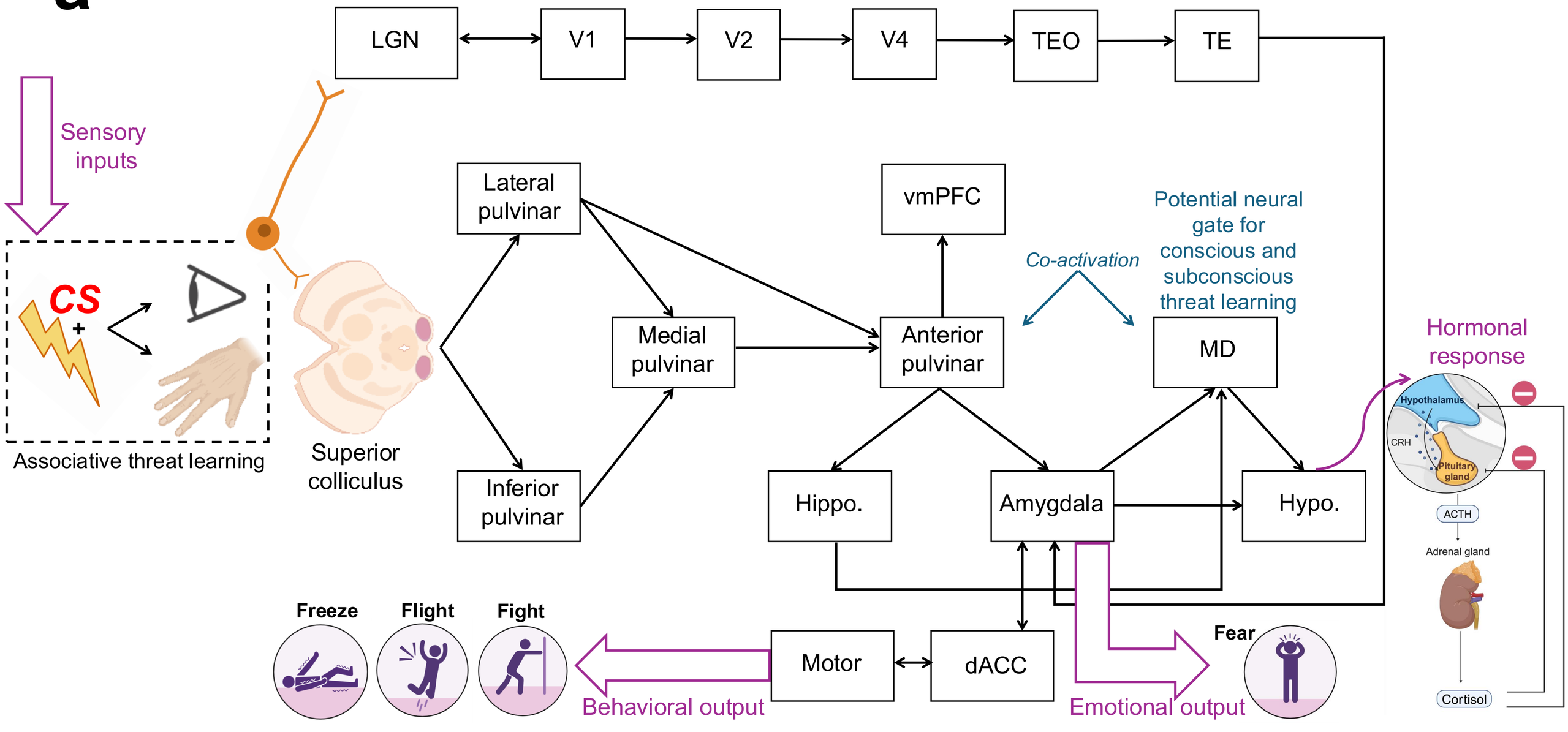
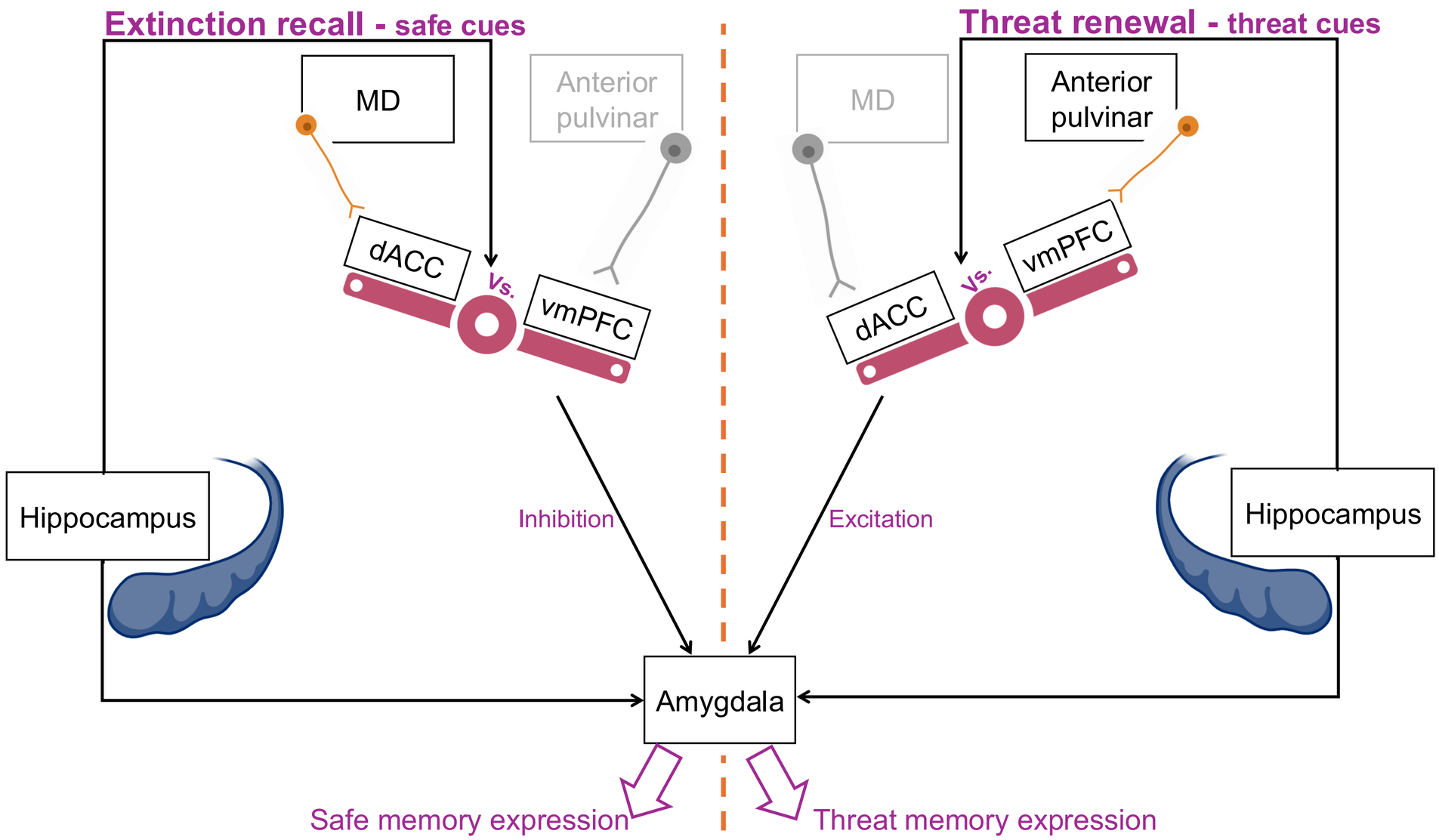
b Dynamic model of safe vs. threat memory retrieval using contextual cues: A thalamic-dependent "toggle switch"